

R/V Heincke (HE431) Report

**HABCYST: Interactions and feedback mechanisms between oceanography,
chemical signatures and microbial ecology, with a focus on HAB species diversity
and activity**

Cruise No. HE431

August 18th – September 9th, 2014

U. John A. Cembella, S. Wohlrab, S. Murray, R. Henkel, , D. Meier, J. U. Kegel, N.
Kühne, S. Westphal, D. Voß, , A. Müller, K. Haslauer

2015

Contents

2	Summary	3
3	Participants.....	5
4	Research Program	6
5	Narrative of the Cruise	6
6	Methodology and Instrumentation.....	8
5.1	Physical oceanography and bio-optics	8
5.1.1	Oceanographic parameters from the ship CTD.....	8
5.1.2	Chlorophyll, SPM and CDOM from water samples	9
5.1.3	Bio-optical parameters from the profiling system.....	10
5.1.4	Underway data from the Ferry-Box and ship systems.....	11
5.1.5	Ocean color sensing	11
5.2	Nutrients and DOM	12
5.3	Toxins.....	13
5.4	Microplankton species diversity.....	14
5.5	Molecular biodiversity.....	16
5.8	Cyst distribution.....	19
6	Preliminary Results.....	20
6.1	Physical oceanography and bio-optics	20
6.1.1	Oceanographic parameters from the ship CTD.....	20
6.1.2	Chlorophyll and CDOM/FDOM from water samples	25
6.1.3	Bio-optical parameters from the profiling system including SPM.....	27
6.1.4	Underway data from the Ferry-Box and ship systems.....	29
6.1.5	Ocean color sensing	29
6.2	Nutrients and DOM	31
6.3	Toxins in field samples.....	35
6.4	Microplankton species diversity.....	35
6.5	Molecular biodiversity.....	36
6.6	Cyst distribution.....	41

6.7	Metatranscriptomics	42
6.8	Viruses	43
7	Station List.....	45
8	Data and Sample Storage and Availability	46
9	Acknowledgements.....	47
10	References.....	48

2 Summary

The HABcyst cruise (Heincke HE431) focused on the detection and analysis of temporal and spatial relationships among members of plankton communities with respect to putative environmental drivers/stressors. The primary transects were along the Norwegian coast, southward from the Lofoten region, including incursion into the major fjords Nordfjord and Sognefjord, then along the southern coast and via Skagerrak into open coastal waters and fjords of the Swedish west coast. Although zooplankton, bacterial and viral components were also examined to some extent, particular attention was targeted towards key phytoplankton genera associated with Harmful Algal Blooms, and more specifically to taxa that are both toxigenic and capable of forming sexual resting cysts, which overwinter in the sediments. During the cruise, the composition of size-fractionated net plankton and Niskin bottle casts from the pelagic zone was analyzed microscopically for species identification and cell quantitation. Subsequently, in the laboratory, ecogenomic DNA sequencing of size-fractions of whole plankton communities was conducted to confirm species diversity and for comparison with microscopic analysis. Attempts were made to link species composition and diversity to biotic and abiotic parameters concurrent with the plankton sampling regime. The interpretation of the diversity patterns of corresponding cellular activities is recognized as crucial to understanding pelagic ecology in fjord systems and to predict the effects of climate change.

In general, microscopic analysis of the micro- and nano-plankton revealed a post-spring bloom community, with low chlorophyll concentrations, low plankton biomass and a relatively high abundance of micrograzers. Expected genera of centric diatoms were present, some pennate diatoms (e.g., *Pseudo-nitzschia* spp.), as well as low abundance of large thecate dinoflagellate (not “bloom” concentrations), such as putatively toxigenic species of *Alexandrium*, *Protoceratium*, *Dinophysis* and *Lingulodinium*. Some of these dinoflagellates were successfully brought into culture and subsequently studied for toxin composition and morphological and molecular diversity. In most cases, the presence of toxins in the plankton could be associated with the prospective source organisms, e.g. PSP toxins with *Alexandrium* cells in Lofoten and *Pseudo-nitzschia* with the detection of domoic acid in Nordfjord. Perhaps surprisingly, very few dinoflagellate cysts were recovered from the surface sediments and almost none of *Alexandrium* were found, in spite of the generally favorable consistency of the substrate (fine sand and silt) for cyst retention. It is likely that excystment and/or massive advection away of vegetative cells had already occurring by the late summer.

The CTD measurements of temperature and salinity profiles essentially matched what would be expected of fjord circulation at this time of year, i.e. high stratification with low surface salinity within the fjords and a sharp pycnocline. An array of bio-optical sensors was deployed to attempt to establish relationships between optical properties of the water masses and resident plankton population, but no clear causal linkages were determined. Typically, higher Chl a concentrations within the Swedish fjords (relative to those in western Norway) corresponded to higher plankton biomass, often dominated by dinoflagellates. Correlation plots

of various parameters showing good correspondence of results by combining CTD, FerryBox, laboratory and profiler data, e.g. for Chl a, turbidity, backscattering. The distribution of macronutrients generally indicated high depletion at the surface, with a typical late summer increased concentration with depth. In terms of DOC and DOM, the highest concentrations were found in Stavanger Fjord and within the Swedish fjord area, generally corresponding to higher plankton biomass, with mixed-layer DOC concentrations higher than in deeper waters, as expected.

Post-cruise analysis of molecular diversity by PCR and with (NGS)-454 amplicon sequencing followed by multi-variate analysis revealed high cryptic diversity as well as high variability among coastal sites and fjord systems. As one example, the nanoplankton within the Lofoten, Nordfjord and Sognefjord were significantly more diverse compared to the Swedish coast and fjords. The HABcyst cruise yielded an abundance of new knowledge on the association of plankton biodiversity in various coastal and fjord systems, and further attempts are now underway to provide the linkage to environmental variables and potential driving forces resulting from climate-driven regime shifts in the Arctic, sub-Arctic and north temperate waters.

3 Participants

	Name	Operation	Institute
1	John, Uwe, Dr.	Chief scientist	AWI
2	Cembella, Allan, Prof Dr.	Scientist, Plankton ecology	AWI.
3.	Kegel, Jessica, Dr.	Scientist , Virus ecology	AWI.
4	Murray, Shauna, Prof Dr.	Scientist, Plankton ecology	UTS, Sydney
5*	Wohlrab, Sylke, Dr.	Scientist, molecular ecology	AWI.
6 .	Kühne, Nancy.	Technician, molecular ecology	AWI.
7	Westphal, Stephanie	PhD student, molecular ecology	AWI
8	Müller, Annegret	Technician, Toxicology/Chemistry	AWI
9	Haslauer, Kristina	HIWI chemistry	AWI
10*.	Fabro, Elena.	PhD student, Plankton ecology	CONICET.
11	Henkel, Rohan	CTD / bio-optics scientist	ICBM
12 .	Voss, Daniela.	CTD / bio-optics scientist	ICBM
13	Meier, Daniela	CTD / bio-optics engineer	ICBM

*Participants exchange at 01.09.2014 in Bergen

Affiliations

AWI: Alfred-Wegener-Institut
Helmholtz-Zentrum für Polar- und Meeresforschung
Am Handelshafen 12, 27570 Bremerhaven, Germany
email: Uwe.John@awi.de

ICBM: Institut für Chemie und Biologie des Meeres
Carl von Ossietzky Universität Oldenburg
Ammerländer Heerstraße 114-118, 26129 Oldenburg, Germany
email: oliver.zielinski@icbm.de

UTS C3: Plant Functional Biology and Climate Change Cluster
University of Technology Sydney
PO Box 123 Broadway, NSW 2007, Australia
email: Shauna.Murray@uts.edu.au

CONICET: Consejo Nacional de Investigaciones Científicas y Técnicas.
Facultad de Ciencias Naturales y Museo de la Universidad de La Plata
Paseo del Bosque s/n. La Palta, Buenos Aires, Argentina.
email: fabroelena@yahoo.com.ar

4 Research Program

The Ecosystem component of the HE431 cruise **HABcyst** addressed interactions and feedback among hydrographic regimes, biogeochemical and bio-optical signatures and phytoplankton species diversity and molecular activities, with a focus on potentially toxigenic species associated with Harmful Algal Blooms (HABs). In particular, we focused on key questions regarding molecular diversity and associated biological activity, via studies of gene expression in defined coastal areas, and potential spreading of selected toxic species along the Norwegian coast. With respect to global change, the objective was to characterize coastal waters for definable marine biodiversity, organic components and marine bio-optical properties, with linkages to the effect of coastal proximity within and adjacent to selected fjord systems. **Detecting and analyzing temporal and spatial phytoplankton communities with respect to the corresponding cellular activities and the environmental driver/stressors is extremely important to understand pelagic ecology in fjord systems and predict the effects of climate change.**

These objectives were addressed by the following specific elements: 1) establishing an inventory of the phytoplankton diversity in various size-fractions; 2) determining metabolic activities of the planktonic communities in different size-fractions and sampling areas; and 3) determining the water chemistry, including the composition of DOM in the water column. By combining data from the oceanographic, biogeochemical and bio-optical components with conceptual modeling, we contributed to major advances in understanding coastal ecosystems with regard to the distribution and dynamics of biodiversity and targeted key species (including HAB taxa) and to the influence of climate change scenarios.

5 Narrative of the Cruise

The research cruise HE431 started on 18.08.2014 at 8:00h in Bremerhaven. We experienced harsh weather conditions and had to continue at reduced speed (3-4 kn) for the first few days while heading northeast towards Norway and north along the coast. The cruise duration was 20.1 days over a total distance of 1170 sm. The cruise terminated when we returned to Bremerhaven on 08.09.2014 at 8:00h.

The overarching aim of this cruise was to study the populations of putatively toxigenic dinoflagellates. This mission aspect was only partially successful due to the late cruise timing and therefore many target species were not abundant in the water column anymore or had even completely gone. We sampled for phytoplankton with a 20 μm mesh plankton net and for nutrients, dissolved organic matter (DOM) and phytotoxins with a rosette sampler equipped with Niskin bottles. In addition to the water column, we also investigated the sediment for potential resting-cyst stages of the key dinoflagellates. These samples are currently under examination.

Lofoten: On 23.08.2014 we reached the first sample station (Table 1). We had nine stations to sample and moved at the 25th to the next transect. The salinity at the surface was around 33.8 and up to 35 in deeper water. The surface water temperature of the first five stations was between 9.5 and 11°C and slightly higher at the entrance of the fjord (station 6). At depth < 7 m the temperature was < 7 °C. Around Lofoten, PSP toxins were detected and measured in the collected cell pellets, corresponding to the presence of cells of *Alexandrium* spp. The most abundant recognizable phytoplankton species in the nano- to micro-plankton were those of *Ceratium*, *Chaetoceros* and *Pseudo-nitzschia*. *Dinophysis* species, as well as of *Alexandrium*, were also present and cells of the latter were isolated into culture.

Nordfjord: The Nordfjord (28.08-29.08.2014) was up to 1000 m deep and exhibited a highly transparent surface layer in the water column. The salinity increased within the first 5 m to up to 30 m. Until 40 m depth, the salinity increased to 34.5 but then did not change further. At the entrance the fjord the surface layer was not as clear. A salinity of 31.8 (surface) to 34.8 (depth) was measured. At the fjord entrance, the temperature was 14.4°C at the surface, decreasing from 20 m to about 10°C and down to 8°C by 30 m, without a further decline with depth. Within the fjord, the surface was 16°C, decreasing at 16m to < 10°C and down to 8°C below 35 m depth. As at Lofoten, *Ceratium* species, but also those of *Pseudo-nitzschia* and *Protoperdinium*, were prominent. We detected domoic acid, the toxin produced by *Pseudo-nitzschia* species, in corresponding plankton samples.

Sognefjord: The Sognefjord is > 1200 m deep and among the deepest and largest fjords in Europe. The fjord showed similar water layering as in Nordfjord, with higher salinity and lower temperature at the outermost station. At the outermost station of the fjord, salinity was 30.8 (15.6°C) and below 47 m the temperature declined noticeably around 10°C (salinity 34.6). With increasing depth only the temperature declined appreciably. Within the fjord, the surface temperature was reached up to 16.7°C and declined from 38 m to 10°C. When entering the fjord this 10°C isotherm shifted to 17 m. At the surface, salinity was 22, but this increased rapidly to 30 (at around 8 m) and increased further to 35 in deeper waters. The microscopically identified plankton community composition was similar to that of the Nordfjord but at higher cell abundances; in this region, *Lingulodinium polyedrum* was found to be prominent, whereas cell numbers of *Pseudo-nitzschia* species were less than in Nordfjord.

On 01.09.2014 we entered the Bergen harbor and exchanged scientists.

Stavanger Fjord: On 2-3.09.2014 sampling of the water column around Stavanger did not show distinct layering. Two stations at the coast were 80 to 140 m deep whereas the stations within the fjord varied in depth from 360m (station 26) to 500m (station 25). The surface temperature was around 17°C and at 100 m temperatures around 10°C. Between these two stations, the salinity was around 26 at the surface, whereas the salinity of the coastline station was around 34. Here we found a relatively homogenous phytoplankton assemblage with few dominant large dinoflagellates, such as *Ceratium* and *Protoperdinium* spp. Only a few cells of *Prorocentrum* and *Alexandrium* were observed.

Swedish Fjord system: The Sweden transect was sampled on 05 – 06.09.14 including an area of several relatively shallow connected fjords and where the greatest depth (30.7 m) was found at station 31. The temperatures at the surface were around 18°C and only declined below 10°C at station 31. The surface salinity of 20 to 22 increased at greater depth, where the highest value (32.9) as measured at 30.7 m at station 31. The phytoplankton diversity was high and the total biomass much higher compared to the other study areas. We found several potentially toxigenic species and even fishing was closed by the local authorities due to occurrence of phycotoxins in the water column.

In summary, after the bad weather conditions during the first week we lost considerable work time, but could adjust the sampling regime and station plan such that most scientific objectives were accomplished. We thereby gained important comparative insights into plankton dynamics and diversity, particularly of HAB taxa, in coastal/fjord systems of Norway and Sweden.

6 Methodology and Instrumentation

5.1 Physical oceanography and bio-optics

(Voß, Meier, Henkel)

6.1.1 Oceanographic parameters from the ship CTD

The CTD casts were performed with a Seabird 'sbe911+' CTD probe with sampling rosette (onboard device) at each station, as an initial activity at the station to determine further key discrete sampling depths, e.g., to locate chlorophyll maxima. Live data acquisition was carried out via CTD-client onboard and data post-processing with Seasoft V2. Salinity and depth were calculated from pressure values (UNESCO, 1983), and temperature was corrected to ITS-90 (Preston-Thomas, 1990). The CTD was equipped with additional sensors for turbidity, fluorescence and oxygen. All CTD data will be published via Pangaea® (www.pangaea.de). A station list and the master track of *R/V Heincke* is already published (doi:10.1594/PANGAEA.837741). CTD data are under process and will be published as soon as possible also linked to already published track.



Figure 1 Onboard device Seabird 'sbe911+' CTD probe with sampling rosette at station work on *R/V Heincke*.

6.1.2 Chlorophyll, SPM and CDOM from water samples

Water samples were collected at each station from defined depths to measure colored dissolved organic matter (CDOM), suspended particulate matter (SPM) and chlorophyll *a* (Chl *a*). Immediately after sampling, CDOM and FDOM samples were filtered under low vacuum through 0.2 μm membrane filters (Sartorius, Germany). The filtration unit had been pre-rinsed with Milli-Q dionized water (Millipore, USA) to avoid contamination, followed by sample water (~100 mL). Samples were directly analyzed onboard.

In a 0.01 m quartz cuvette, pre-rinsed twice with filtered seawater, both absorbance spectra and fluorescence excitation-emission matrices (EEM) for FDOM were measured with a spectrofluorometer (Aqualog®, Horiba Scientific, Germany). Measurements were performed using Milli-Q water as reference. The scan ranged from 240 to 600 nm with an excitation increment of 2 nm, an emission increment of 0.8 nm, and an integration time of 2 s. From these data, the absorption coefficient $a(l)$ was derived at wavelength l according to $a(l) = 2.303D(l)/L$, where L is the path length in meters and D the absorbance measured by the instrument. The EEM data were scanned for peaks according to Coble (2007).

Additionally, CDOM absorbance was measured in 0.1 m quartz cuvettes with a UV-VIS-spectrophotometer (UV-2700, Shimadzu). Samples were scanned at medium scan speed with an increment of 0.5 nm in the spectral range between 200 nm and 800 nm. Ultrapure water (Milli-Q) was used as reference. Sample and reference cells were pre-rinsed twice with sample and purified water before analysis. Absorbance values $A(\lambda)$ were baseline corrected and converted to the absorption coefficient $a_{\text{CDOM}}(\lambda)$ [m^{-1}] following $a_{\text{CDOM}}(\lambda) = 2.303 \times A(\lambda)/L$, where λ is the wavelength and L is the path length of the cuvette in meters.

For SPM determination, water samples (in triplicate, up to 10 L volume) were filtered through pre-combusted and pre-weighed Whatman GF/F filters, pre-washed and rinsed with Milli-Q water. Filters were frozen immediately at -25 °C and reweighed in the laboratory after the cruise. The SPM concentrations were normalized to 1 L.

Chl *a* was determined (in triplicate, up to 1 L volume) after sample filtration through pre-combusted Whatman GF/F filters, pre-washed and rinsed with 0.2 μm filtered seawater. Filters

were stored onboard at -25°C and analyzed later in the laboratory after pigment extraction with acetone followed by fluorometric measurements and calculation of chlorophyll a concentrations according to EPA method 445 (Arar & Collins, 1997).

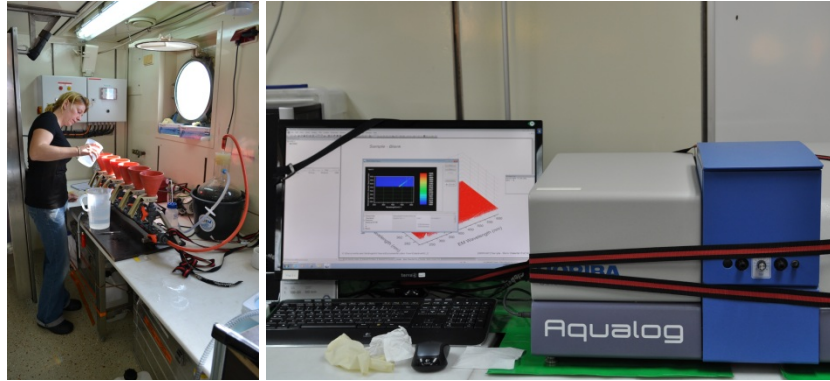


Figure 2 Filtration onboard *R/V Heincke* to determine Chl a and SPM (left). Aqualog[®] spectrofluorometer to determine absorbance spectra and fluorescence excitation-emission matrices (EEM) for CDOM/FDOM.

6.1.3 Bio-optical parameters from the profiling system

A HyperPro II profiling system (Satlantic, Halifax, Canada) was used to acquire bio-optical data for different parameters. The profiler consists of one hyperspectral irradiance and one hyperspectral radiance sensor, as well as fluorescence and backscatter sensors and an integrated CTD. A second hyperspectral irradiance sensor was mounted on the research vessel for reference measurements. On the profiler, the irradiance sensor measures downwelling and the radiance sensor upwelling light. The fluorescence sensors measure chlorophyll, CDOM, phycoerythrin and phycocyanin fluorescence signals. The backscatter sensor retrieves data at 470 nm and 700 nm.

Profiler measurements were conducted at selected stations depending on sea and weather conditions. At these stations, three casts were typically performed. At each cast, the profiler was lowered until the downwelling light values were of the same order of magnitude as the background noise level of the sensor.

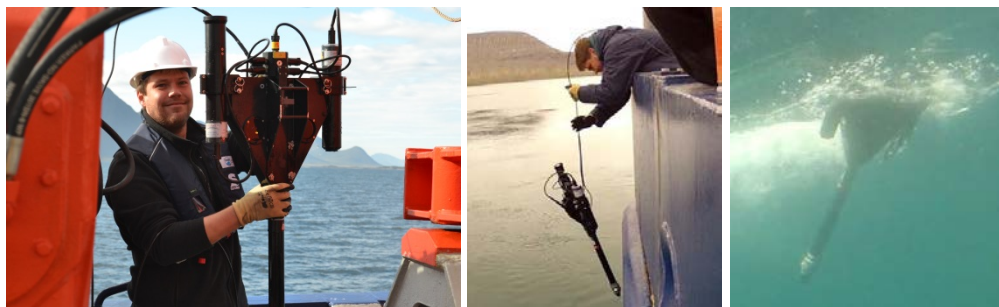


Figure 3 Hyperspectral profiling system Satlantic Inc. (Canada) to determine bio-optical data during free fall mode from of *R/V Heincke*.

6.1.4 Underway data from the Ferry-Box and ship systems

The PocketFerryBox is a flow-through system deployed as an underway device for ship expeditions and for attendant measurements during stationary operations. The system provides basic data at high spatial and temporal resolution for various parameters, e.g., salinity, temperature (at the intake and inside the system), chlorophyll-fluorescence, CDOM-fluorescence, turbidity, dissolved oxygen. An additional advantage is the expandable design of the system to integrate further sensors. On this cruise, a second box was equipped with a UV- and a VIS-spectrophotometer, e.g. for optical nitrate measurements, and to improve current processing algorithms. For multi-parameter sensing, water was pumped from the moonpool of the ship. Measurements were performed at a sampling interval of 1 min.



Figure 4 PocketFerryBox (right) with AddOn box equipped with UV-/VIS spectrometers (left).

6.1.5 Ocean color sensing

Secchi depth & Forel-Ule observations

Water transparency measurements were performed with a 30 cm Secchi disc at each daytime station to determine the penetration of light. The Forel-Ule (FU) color comparator scale is a device that is composed of 21 colors, from 'indigo blue' to 'cola brown', and represents the range of colors that can be found in the open sea, coastal, and continental waters. Based upon a historical background, this provides an estimation of the present water constituents influencing the water color. The color of the water was determined over a Secchi disc at half the disc's depth (where the disc disappears from sight) at each day station.



Figure 5 Secchi disc above and in water (left, middle) and Forel-Ule (FU) color comparator scale to determine the water color (right).

Hyperspectral radiometric observation

Above-water hyperspectral radiometric observations were conducted during the whole cruise. A radiometer setup with a RAMSES-ACC hyperspectral cosine irradiance meter to measure $ES(\lambda)$ (downwelling solar irradiance), and two RAMSES-ARC hyperspectral radiance meters (one set-up at starboard, one at the port side of the ship) to measure $L_{sfc}(\theta_{sfc}, \Phi, \lambda)$ (upwelling water-leaving radiance) and $L_{sky}(\theta_{sky}, \Phi, \lambda)$ (sky-leaving radiance) were installed on the ships foremast (TriOS GmbH, Germany). Hyperspectral measurements were collected at 5 min intervals over a spectral range $\lambda = 320 - 950$ nm. Data processing was done according to Garaba & Zielinski (2013).



Figure 6 Radiometric set-up on the foremast of R/V Heincke. One RAMSES-ACC hyperspectral cosine irradiance meter was installed at the top of the mast to measure total downwelling solar irradiance (red circle).

5.2 Nutrients and DOM

(Westphal, Burau, Krock)

Every station was sampled (except for sediment stations 10-12) for dissolved organic carbon (DOC), solid-phase extracted organic matter (SPE-DOM) and nutrients from various depths.

Nutrients

Subsamples of seawater were directly collected from the Niskin bottles of the CTD-rosette-system and stored at -20°C until further analysis in the laboratory. Nitrate, nitrite, ammonium, phosphate and silicate were measured with an autoanalyzer system (Evolution III, Alliance instruments) by standard seawater methods (Kattner and Becker 1991). All samples were analyzed in duplicate; the accuracy was set by running three standards at the beginning and two standards after each 8 samples. The analytical precision of replicates was approximately 0.05 µM for nitrate, silicate and ammonium and 0.01 µM for phosphate and nitrite for the range of concentrations in this study.

DOM extraction and molecular characterization

The DOC concentration of the original glass fiber-filtered samples (Whatman GF/F, pre-combusted at 450°C for 5 h) was determined by high temperature catalytic oxidation (TOC-V_{CPN} analyzer, Shimadzu). For SPE-DOM measurements, subsamples of the filtrates were acidified to pH 2 with HCl (32%, p.a.) and passed through SPE cartridges (PPL, Varian), rinsed with acidified ultrapure water. The SPE-DOM was eluted with methanol according to Dittmar et al. (2008). The SPE-DOM fraction was roughly characterized according to its polarity distribution in a water/methanol gradient by reverse-phase liquid chromatography (Koch et al., 2008). In addition, samples will be analyzed with an FT-ICR mass spectrometer (Apex Qe, Bruker Daltonics, Billerica, MA), equipped with a 12 T refrigerated actively shielded superconducting magnet (Bruker Biospin, Wissembourg, France). An Apollo II dual electrospray source (ESI, Bruker) will be used in negative ion mode (for details see Lechtenfeld et al., 2013).

5.3 Toxins

(Müller, Haslauer, Cembella, Krock)

Toxin extraction from plankton

Cell pellets from the plankton net tows were harvested by centrifugation, suspended in 500 µL methanol for lipophilic toxins or 0.03 M acetic acid for hydrophilic toxins, and subsequently extracted by homogenization and then filtered. Polycarbonate filters with 20 µm prescreened samples from the rosette bottles were repeatedly rinsed with 1 mL methanol until complete decoloration of the filters. The methanolic extracts were filtered and analyzed by tandem mass spectrometry.

Liquid chromatography with fluorescence detection (LC-FLD)

Hydrophilic paralytic shellfish poisoning (PSP) toxins were determined by liquid chromatography with fluorescence detection (LC-FLD). Aqueous extracts were analyzed by reverse-phase ion-

pair liquid chromatography and post-column fluorescence derivatization, following minor modifications of previously published methods (Diener et al. 2006, Krock et al. 2007). The LC-FLD analysis was carried out on a LC1100 series liquid chromatography system equipped with a Phenomenex Luna C18 reversed-phase column (250 mm X 4.6 mm id, 5 μ m pore size) precolumn. The column was coupled to a PCX 2500 post-column derivatization system. The injection volume was 20 μ L and the autosampler was cooled to 4°C. The eluate from the column was oxidized with periodic acid before entering the 50°C reaction coil, after which it was acidified with nitric acid. The toxins were detected by dual-monochromator fluorescence (λ_{ex} 333 nm; λ_{em} 395 nm).

Liquid chromatography with tandem mass spectrometry (LC-MS/MS)

Determination of domoic acid and lipophilic toxins in field samples was performed by LC-MS/MS on board. Mass spectral experiments were carried out on a triple quadrupole mass spectrometer coupled to an Agilent model 1100 LC. After injection of 5 μ L of sample, toxins were separated by reverse-phase chromatography on a C8 phase with gradient elution by water and acetonitrile. The chromatographic run was divided into 3 periods for: 1) domoic acid; 2) gymnodimine and spirolides, and 3) okadaic acid, dinophysistoxins, pectenotoxins, yessotoxin and azaspiracids. Selected reaction monitoring (SRM) experiments were carried out in positive ion mode (Krock et al., 2013).

5.4 Microplankton species diversity

(Cembella, Murray, Fabro)

At every station plankton was sampled by vertical net tows through the upper 30m water column by a 20 μ m-mesh net. Plankton communities were characterized by onboard microscopic examination of live or freshly preserved subsamples of these net tows. Crude microscopic observation of live material was first conducted with a stereo-dissecting microscope (Leitz), followed by more intensive examination at higher magnification with contrast interference (Normarski) optics (Lietz Aristoplan). Diluted net tow subsamples were fixed with Lugol's iodine solution and also with buffered paraformaldehyde. The major objectives of the net tow analysis were to establish species dominance, detect the presence of putatively toxigenic species, provide cell enumeration for quantitative analysis of toxin composition and identify rich samples for cell isolation of target HAB taxa from the microplankton community.

In addition, Niskin bottle samples were analyzed for identification and enumeration of key taxa and to check the nanoplankton community for the presence of small potentially toxic species, e.g., of the dinophycean genus *Azadinium*. For this purpose, 1 L samples were gently

concentrated on 5 μm pore-size polycarbonate filters and inspected with an inverted microscope (Leitz Diaplan). At every station, 50 mL bottle-samples were fixed with Lugol's iodine solution (1% final concentration) for quantitative plankton analysis.

When species of interest were detected in the net tow plankton, single cells were isolated by microcapillary pipette into single wells of 96-well plates. Plates were incubated on-board at 10°C and at 50 $\mu\text{mol photons m}^{-2} \text{s}^{-1}$ photon flux density. After the cruise, plates were brought back to the laboratory and processed for clonal culture establishment.



Figure 7 Harvesting of surface plankton by vertical net tow (20 μm -mesh) and subsequent analysis of net tow concentrate by stereo dissecting and phase interference (Nomarski) microscopy.

5.5 Molecular biodiversity

(Westphal, Kühne, John)



Figure 8 Seawater sampling devices used for size fractionation during the cruise

Three net tows (20 μm mesh size, 50 cm diameter) were carried out from 30 m depth, with the net raised to the surface at 0.5 m s^{-1} . Cells larger than 20 μm were collected from the cod-end, rinsed with 0.2 μm -filtered seawater, adjusted to 3 L with sterile-filtered seawater and fractionated through a sequential filtration-tower (200 μm , 50 μm and 20 μm). Additional water was collected from 3, 15 and 30 m depth in Niskin bottles with the rosette sampler then collected into 60 L tanks and filtered through the filter tower (200 μm , 50 μm and 20 μm). The water was collected and further filtered through 3 μm (for nanoplankton) and 0.4 μm (for viruses) or 0.2 μm (picoplankton and bacteria) filters mounted on tripods.

For the net tow and the Niskin bottle samples, the size-fraction retained on 20 μm Nitex mesh (for microplankton) was rinsed off with sterile-filtered seawater and transferred into centrifugation tubes. The centrifugation tubes were topped off to a total volume of 45 mL and split into four 15 mL centrifugation tubes for further analyses (RNA and DNA). The tubes for DNA and RNA-extraction were centrifuged and the supernatant was discarded. The pellet was resuspended in 400 μL 60°C warm AP1 lyse-buffer (DNA) or 400 μL 60°C warm Tris-Reagent (RNA) and transferred into a 2 mL cryovial with three small spatula-tip aliquots of acid-washed glass beads and stored at -80°C until further analysis. Filters from the tripods were cut into four pieces (2 for DNA; 2 for RNA), transferred to a centrifugation tube and rinsed with 1 mL AP1 lyse-buffer (DNA) or 400 μL Tris-Reagent (RNA) and transferred into a 2 mL with three small spatula-tip loads of acid washed glass beads and stored at 80°C until further analysis.

For the micro- and nano-plankton fractions, DNA extraction was performed with the DNeasy® Plant Kit [Qiagen, Hilden, Germany], after adapting the protocol for DNA isolation from dinoflagellates. Picoplankton DNA was extracted as Genomic DNA, using the soil-kit to obtain DNA from eukaryotes and bacteria (Macherey-Nagel, 2011).

PCR and sequencing

The species specific primer pair Dir-F (5'-ACC CGC TGA ATT TAA GCA TA-3') / Dir2-CR (5'-CCT TGG TCC GTG TTT CAA GA-3') and the 341f (5'-CCT ACG GGN GGC WGC AG-3')/ 785rev (5'-GAC TAC HVG GGT ATC TAA TCC-3') primer pair were used for eukaryotes and bacteria, respectively. For the 454-amplicon approach, the universal primers were modified by adding adaptor sequences for the 454-sequencing protocol. The PCR was carried out in 20 µL with the fusion PCR reaction mix on a MasterCycler PCR cycler (Eppendorf, Hamburg, Germany). The resulted amplicons (DNA) were purified with the Qiagen MinElute® kit (Qiagen, Germany) and in a second step with AMPure® beads (Beckman Coulter, USA). To confirm that the amplicons for sequencing were in the expected size range representing the D1/D2 region of the LSU, library qualities were assessed with the High Sensitivity DNA chip on an Agilent 2100 Bioanalyzer (Agilent, Germany). The generated libraries were quantified with RL-Standard (provided in the kit) using the QuantiFluor (Promega, Germany). For all sequencing runs, 20 x 10⁷ molecules were used for the emulsion PCR, carried out with a MasterCycler PCR cycler (Eppendorf, Germany). Sequencing was performed unidirectionally with the GS Junior Titanium Sequencing Kit (Roche, Germany) under standard conditions. The 454 Sequencing System Software version (v) 2.7 was applied with default parameters, i.e., Signal Intensity filter calculation, and Primer, Valley, and Base-call Quality Score filters were all enabled.

5.6 Metatranscriptomics:

(Wohlrab, John)

Plankton samples were taken as described above (see 5. 5: Molecular Biodiversity). Total RNA was extracted on board out of the TriReagent containing cell suspension according to the manufacturer's protocol (Sigma-Aldrich, Steinheim, Germany) with minor protocol adjustments i.e. the addition of liner acrylamide (10-20 µg/mL, Applied Biosystems by Thermo Fisher) and 1/10 volume of 3 M sodium-acetate (pH 5,2-5,5; Ambion by Thermo Fisher) during the precipitation step. The precipitation duration was 2h for microplankton samples and overnight for nanoplankton samples due to the lower biomass in the respective size fraction. Obtained and ethanol washed (twice) RNA pellets were eluted in molecular grade water and stored at -80°C until further downstream processing. The quality and quantity of the RNA was determined with a NanoDrop ND-100 spectrometer (PeqLab, Erlangen, Germany) and a RNA Nano Chip assay on a 2100 Bioanalyzer device (Agilent Technologies, Böblingen, Germany). Aliquots of the RNA samples from stations of interest were subject to Illumina RNASeq sequencing. Obtained libraries were assembled into a reference metatranscriptome with the CLC Genomic Workbench (www.clcbio.org) software. The assembled metatranscriptome was then firstly annotated with the Trinotate software environment and afterwards, the assembled transcripts were assigned to phylogenetic affiliation by BLAST search using a custom BLAST database constructed from reference transcriptomes available from the "The Marine Microbial

Eukaryotic Transcriptome Sequencing Project (MMETSP, Keeling et al. 2014). Finally, the reads obtained from each sequenced sample were mapped against the reference metatranscriptome to obtain gene expression information. The results covering information about expression, identity and function of a respective contig within the metatranscriptome got merged and evaluated with the R software environment implemented with the MANTA package (Marchetti 2015).

5.7 Virus Diversity and Isolation (Kegel, John)

Virus concentrates were generated while onboard *RV Heincke* during the He431 cruise. Water samples (2-3 L) were pre-filtered through 0.45 μm pore-size polycarbonate filters (142-mm diameter, Millipore). The virus-size fraction was concentrated to ~ 50 mL using a VivaFlow 200 (Figure 9) with a 50 kDa MW cutoff filter cartridge (Sartorius). Virus concentrates were stored in the dark at 4°C until further use.



Figure 9 Concentration of viruses using a VivaFlow 200 (Sartorius).

PCR and sequencing and data processing processed at the institute

In brief, PCR was done directly on concentrated seawater samples and set-up in a total volume of 20 μL . All PCRs were done in triplicates and checked on 0.8% agarose gels. Amplicon quantity and quality of the mixed pool was analyzed by an Agilent Bioanalyzer and sequenced with 454 sequence technology using standard protocols (see above). Demultiplexing and OTU clustering of the mcp sequence reads were done with the Qiime pipeline according their MID barcode. OTUs were compared against the nucleotide database using BLAST.

Virus isolation

In order to isolate potential viruses infecting the haptophytes *Prymnesium parvum* and *P. polylepis* 1 mL of the concentrated virus samples was added to an exponentially growing culture. Infected cultures were observed for 14 days for potential lysis.

5.8 Cyst distribution

(Cembella)

Benthic sediment samples were collected (when possible) with a Van Veen-type sediment grab sampler (Figure 10), to examine the abundance and distribution of sexual cysts, of marine dinoflagellates along the cruise track. These cysts represent the dormant resting stage of the life history of many planktonic species, in particular of certain large thecate dinoflagellates associated with HABs. Stations were selected based upon inferences of expected cyst abundances from historical knowledge of the location of blooms of cyst-forming HAB species, expectations of the nature of the sedimentary regime (e.g., sandy, gravelly, or silty) and water depth. Casts were sometimes repeated in cases where the initial cast was only partially successful in retrieving sediments. Mini-cores of the sediment substrate were collected in 50 ml Falcon tubes, and examined microscopically within several hours of collection. Preliminary processing involved dilution of the sediment suspension with a 10:1 V:V ratio of seawater to sediment. The slurry was vortex mixed for several seconds and then shaken vigorously to disaggregate the cysts from sediment particles, then allowed to sediment until the supernatant was clear. The surface layer was aspirated by Pasteur pipette and transferred dropwise to a glass depression slide for microscopic analysis by contrast interference (Normarski) optics (Lietz Diaplan). Samples exhibiting high numbers of cysts of target species, e.g., *Alexandrium* spp., were noted for future isolation of cysts for germination in culture. Whole sediment samples were stored in the dark at 4°C for further processing. Analyses of promising samples is still pending.



Figure 10 Deploying a Van Veen sediment sampler near Disko Bay, Greenland, similar in design to that used to collect sediments from the Norwegian coast aboard *RV Heincke HE431*.

6 Preliminary Results

6.1 Physical oceanography and bio-optics

6.1.1 Oceanographic parameters from the ship CTD

In this chapter the CTD profiles for the coast of Norway and the Swedish sampling area are shown. For all sections, temperature, salinity, and oxygen profiles are plotted over the distance of each station [km].

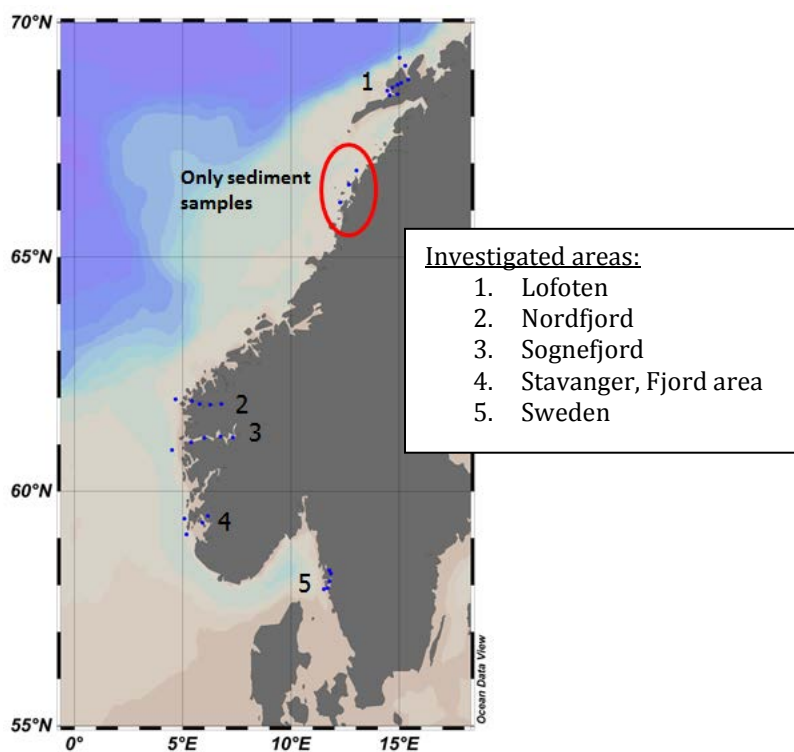


Figure 11 Map of the investigated areas during the cruise HE431 aboard *R/V Heincke*. Within the fjord systems of Nordfjord, Sognefjord and the Swedish Fjords an overall set of 5 stations each were sampled.

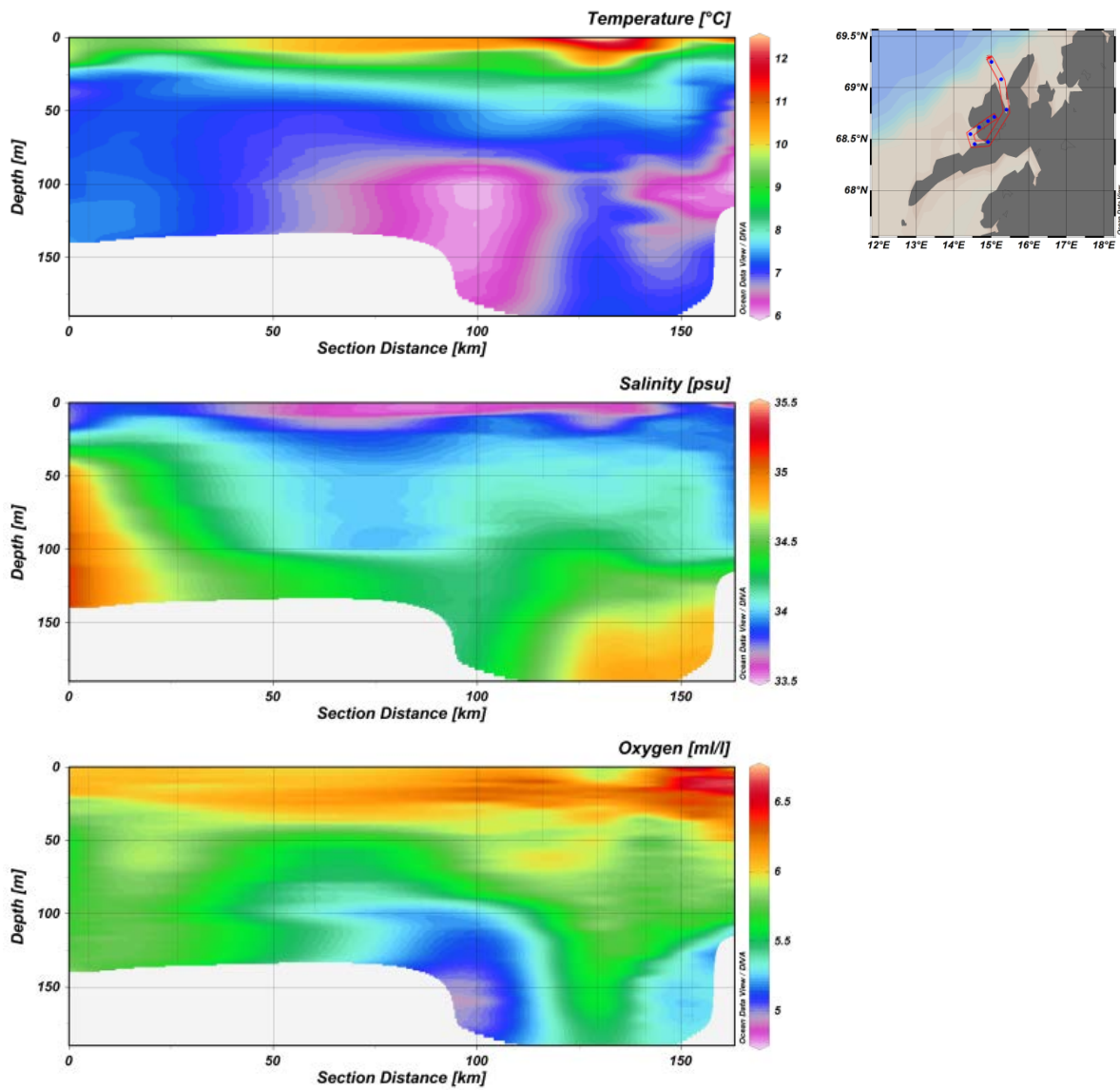


Figure 7 Map of the investigated Lofoten area and associated CTD profiles for full depth over the section distance (km) (from outside to inside stations) for temperature [ITS-90, °C], salinity, and oxygen [mL/L].

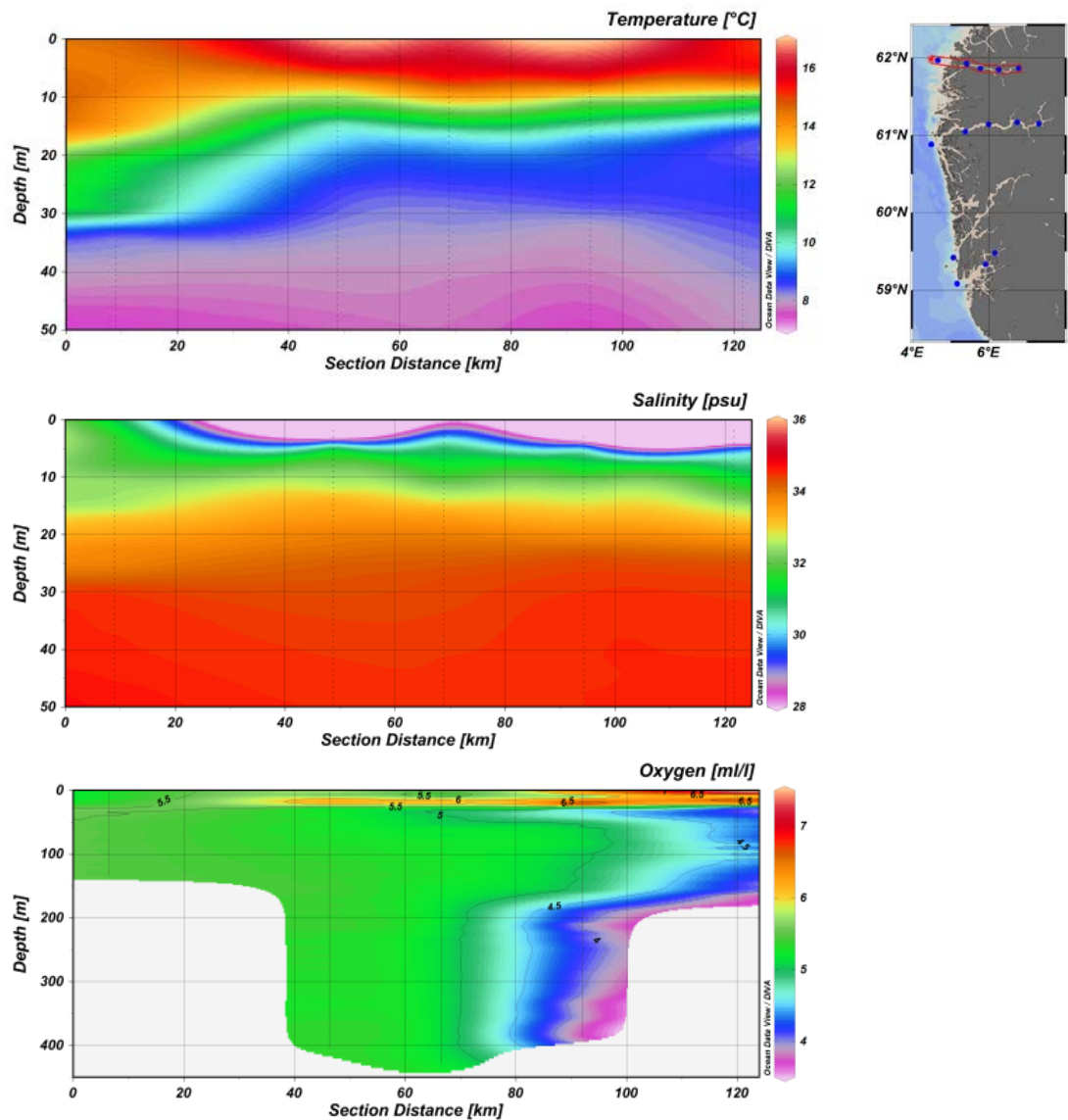


Figure 8 Map of the investigated Nordfjord area and associated CTD profiles over the section distance (km) (from outside to inside stations) for temperature [ITS-90, °C], salinity, and oxygen [mL/L]. Temperature and salinity are shown for the upper 50 m, no significant changes were observed for deeper waters. Oxygen values are shown over the full depth.

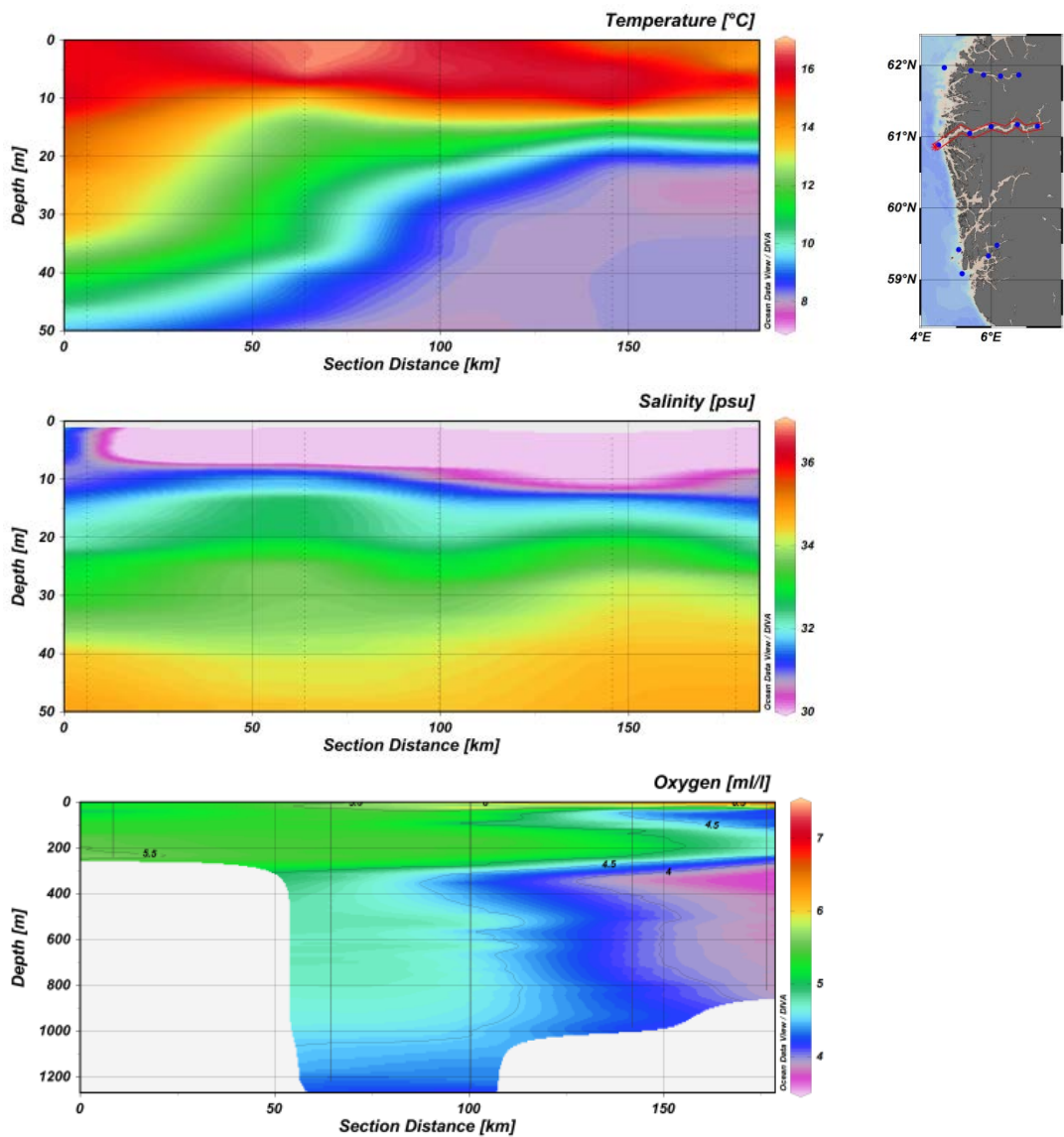


Figure 94 Map of the investigated Sognefjord area and associated CTD profiles over the section distance (km) (from outside to inside stations) for temperature [ITS-90, °C], salinity, and oxygen [mL/L]. Temperature and salinity are shown for the upper 50 m, deeper no significant changes were observed. Oxygen values are shown over the full depth.

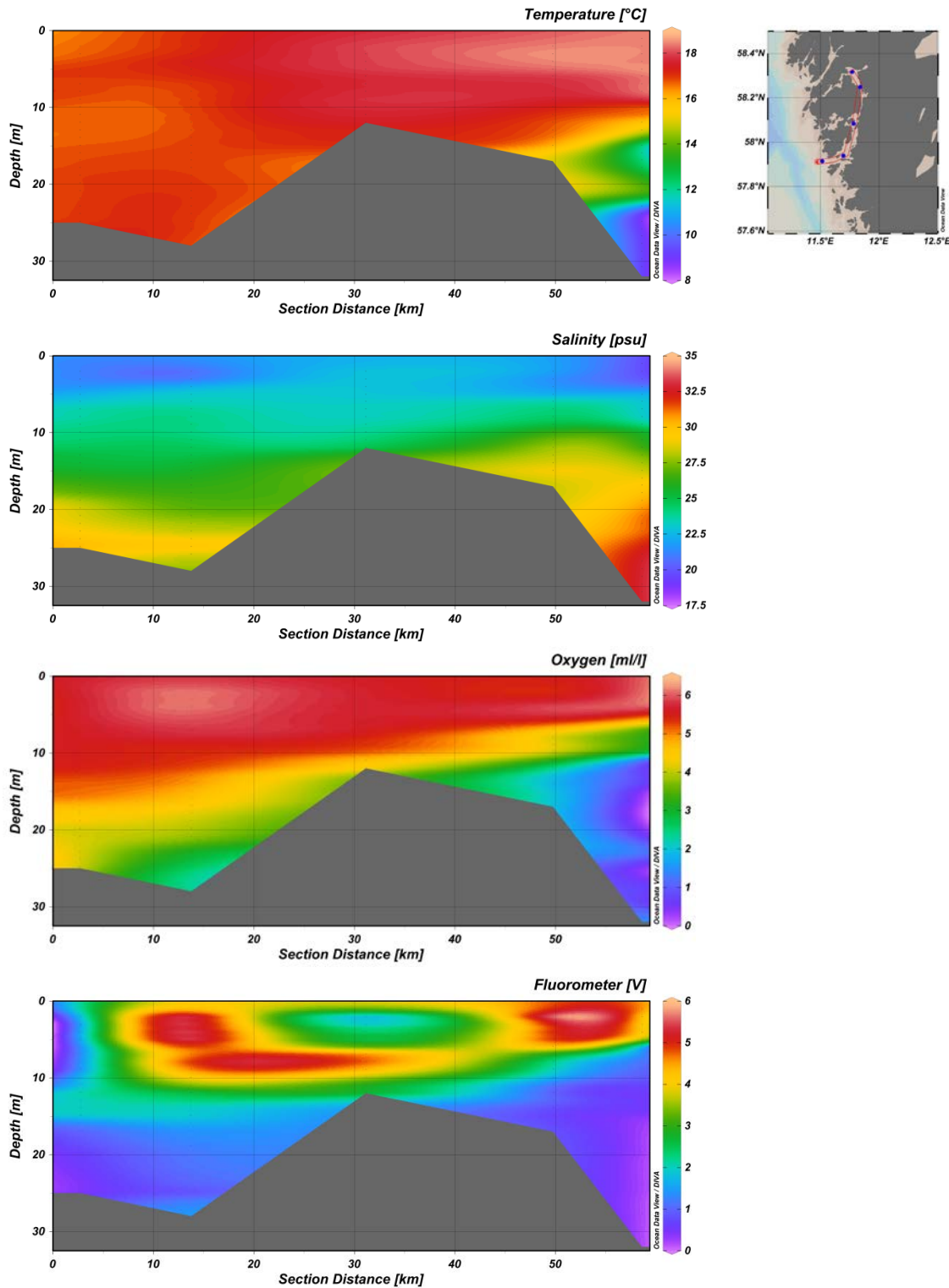


Figure 105 Map of the investigated area at Sweden and associated CTD profiles over the section distance (km) (from outside to inside stations) for temperature [ITS-90, °C], salinity, oxygen [mL/L], and fluorescence.

Comparison of both probes of the CTD for temperature and salinity showed good agreement over the whole cruise.

6.1.2 Chlorophyll and CDOM/FDOM from water samples

Chlorophyll *a*

Results of laboratory analyses of Chl-*a* concentration are shown in Figure 14. Highest concentrations were determined in the Swedish fjord system. Chlorophyll *a* data are one basis for light field modeling, as well as an indicator for phytoplankton biomass.

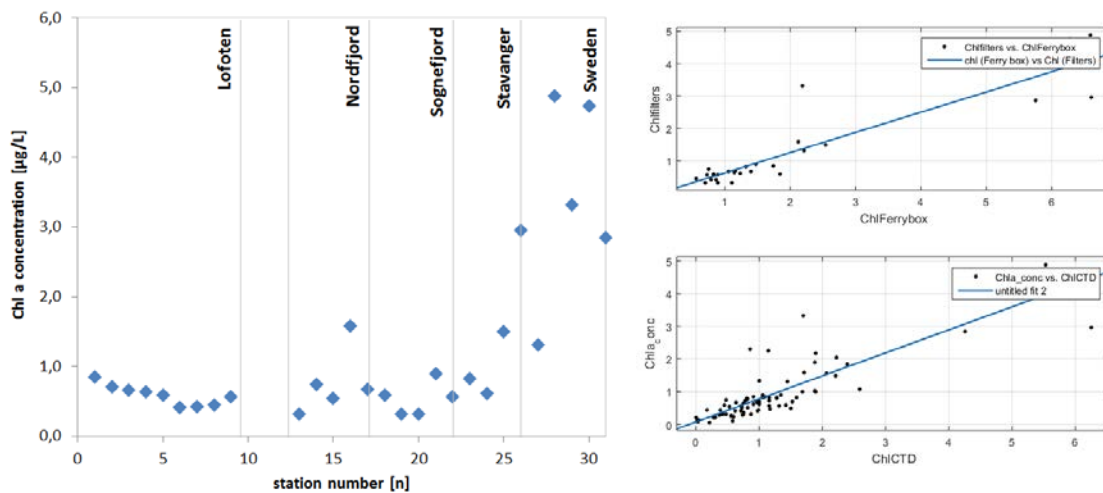


Figure 116 Chlorophyll *a* concentrations over all station of the cruise from 3 m depth. Highest concentrations of Chl *a* were found within the Swedish fjord system (left). Laboratory fluorometric analysis versus optical measurements (FerryBox, $n = 28$, $R^2 = 0.82$; CTD, $n = 78$, $R^2 = 0.72$, with 3, 15 and 30 m) showed good correspondence (right).

CDOM/FDOM

Absorption coefficients of defined wavelengths and Coble peaks over the whole spectral range were determined from absorption and fluorescence data (excitation;emission matrices, EEM compare Figure 15). FDOM Peaks were analyzed for water samples from 3 m depth for main peak components (Figure 16). A comparison between FDOM peaks as well as CDOM absorption coefficients and DOC concentrations will be done in further analysis.

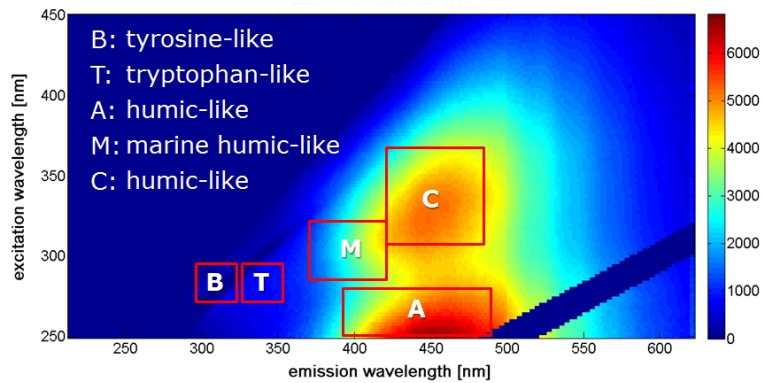


Figure 127 Example of an EEM indicating the important peak areas according to Coble.

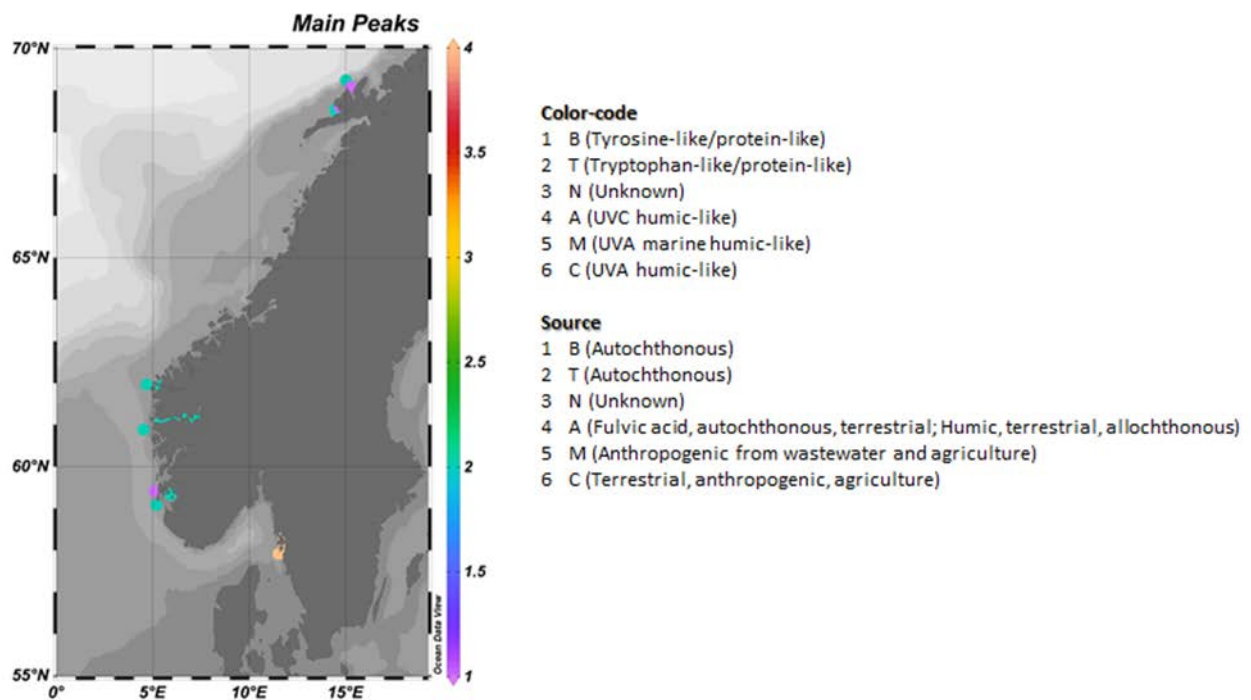


Figure 138 FDOM main peaks in water samples from 3 m depth. Especially tyrosin- and tryptophan-like components (1/2, peak B and T) were mainly found along the Norwegian coast and in fjords, whereas humic-like components (4, peak M) were dominant in the Swedish waters of the cruise.

6.1.3 Bio-optical parameters from the profiling system including SPM

At all daytime station free-falling profiler measurements were conducted to determine light penetration in the water column. A comparison of two stations in Sognefjord is shown in Figure 16. Station 18 represents an outer fjord station whereas station 21 is at the end of the Sognefjord.

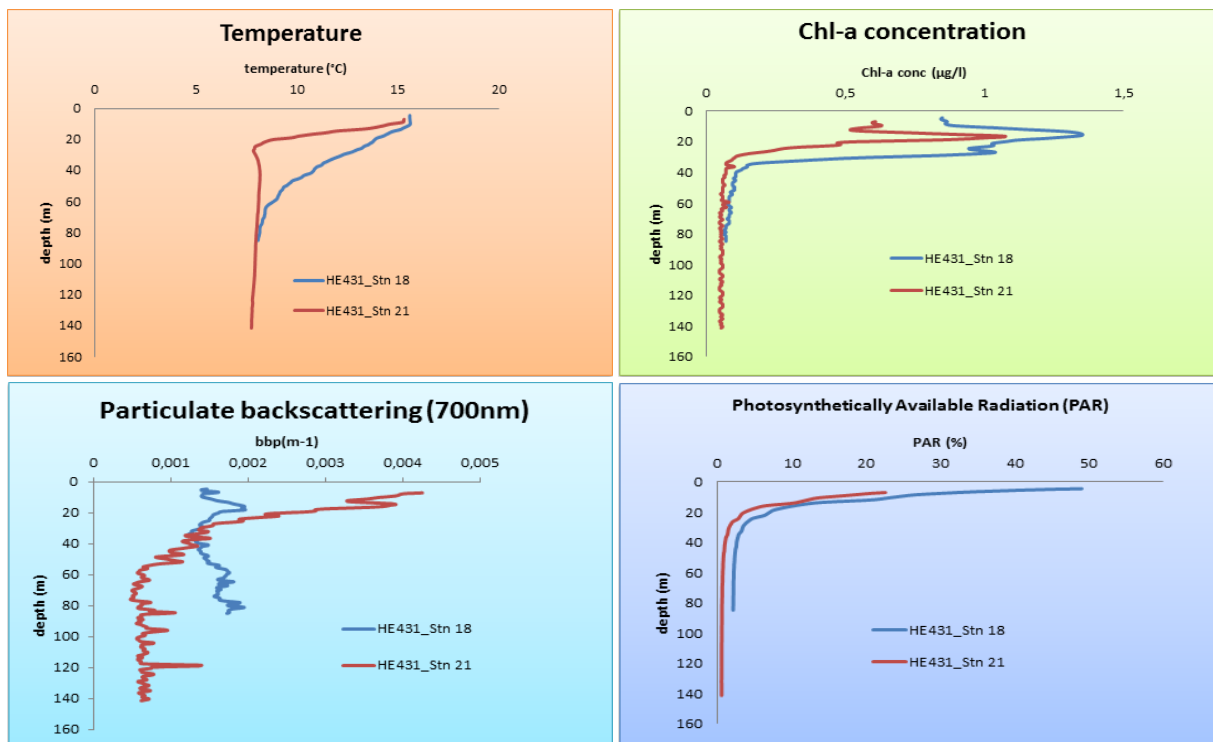


Figure 149 Comparison of two selected profiler stations in the Sognefjord. Station 21 was more stratified with higher backscattering due to particles in the water column. The 1% PAR depth for station 18 was > 85 m, but at station 21 this occurred at 39.5m.

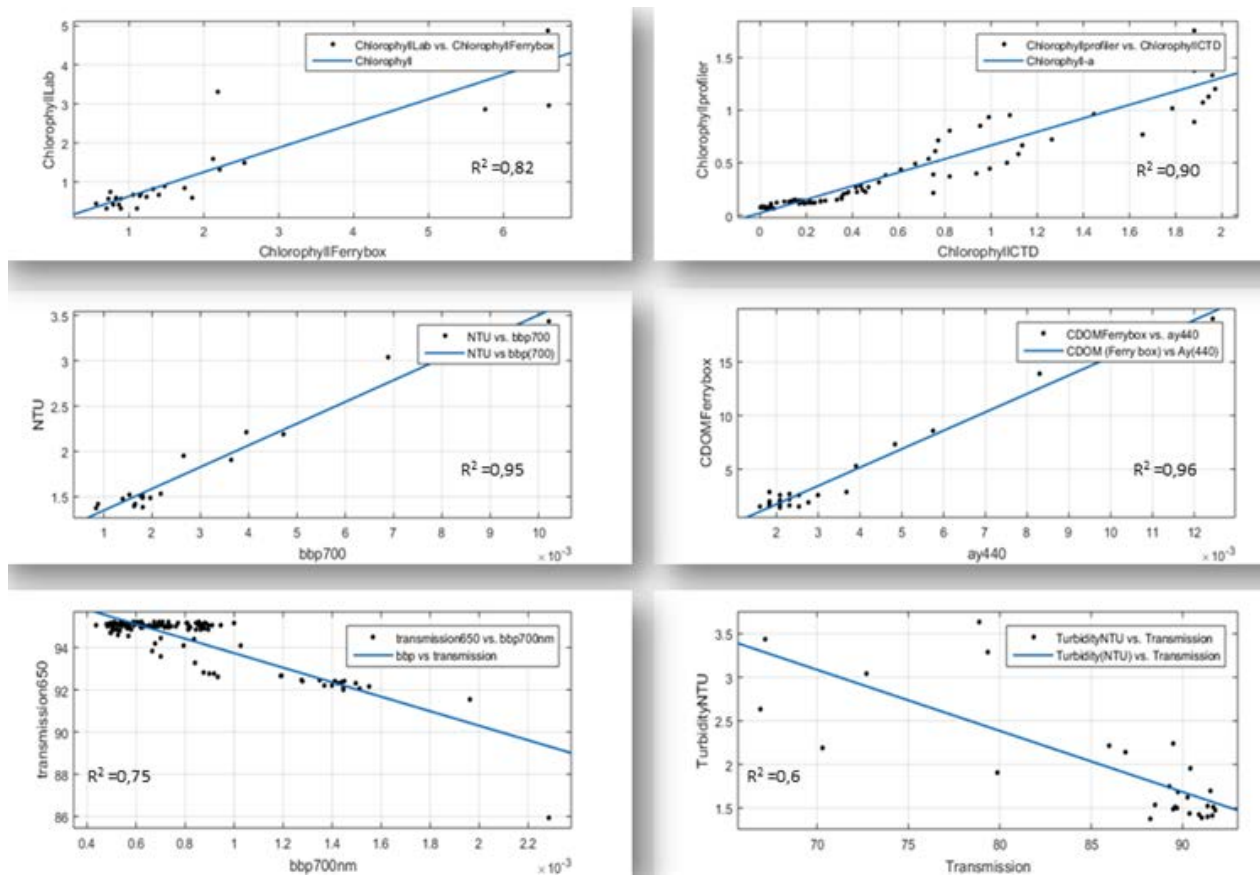


Figure 20 Correlation plots of various parameters showing good correspondence of results by combining CTD, FerryBox, laboratory and profiler data. Chl *a* (lab results) versus FerryBox Chl *a* (upper panel, left); Chl *a* (profiler data) versus Chl *a* (CTD data; upper panel, right); turbidity (FerryBox data) versus backscattering bbp_{700} (profiler data, middle panel, left); CDOM (FerryBox data) versus absorption coefficient a_{440} (lab results, middle panel, right); transmission (CTD data) versus backscattering bbp_{700} (profiler data, lower panel, left), and turbidity (FerryBox data) versus transmission (CTD data, lower panel, right).

6.1.4 Underway data from the Ferry-Box and ship systems

Acquisition of continuous flow-through measurements for various parameters worked very well along the whole cruise track. Results for surface waters for temperature at the intake, salinity, and ~~Chl~~Chl*a* fluorescence are shown in Figure 19.

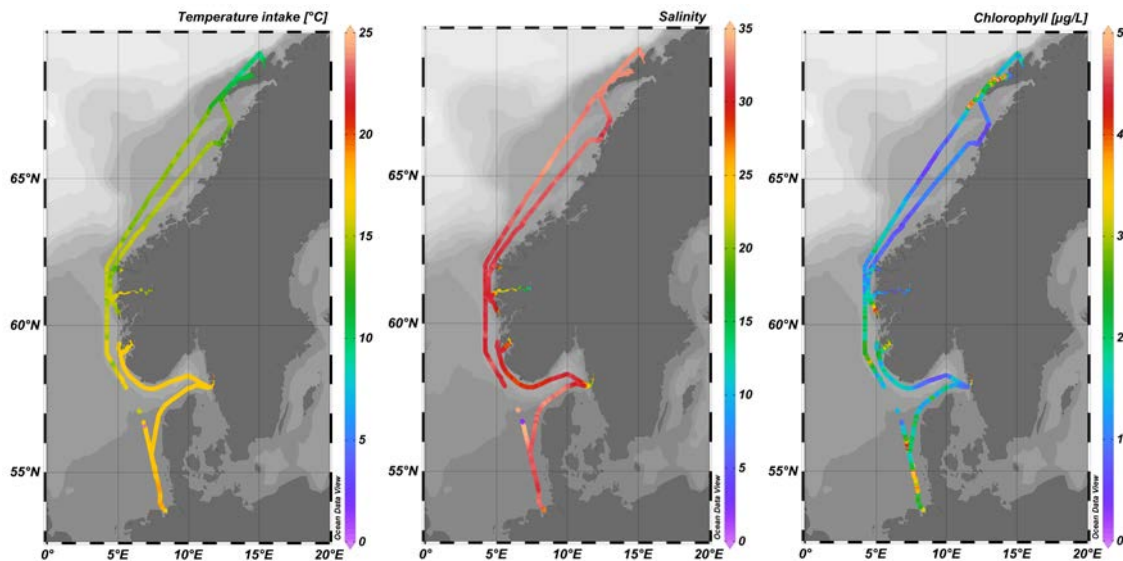


Figure 15 Temperature, salinity, and Chl *a* from FerryBox investigations in surface waters over the whole cruise track.

6.1.5 Ocean color sensing

Results from the Secchi disc measurements can be seen in Figure 20 (left). Highest penetration depths were recorded for the Norwegian stations, with values up to 14 m. The results of Forel-Ule indices (FUI) are shown in Figure 20 (right), representing open sea and coastal regions. High penetration depths correspond well with lower FUI values, clearly seen in the Swedish fjord system (Figure 21). With further processing, more conclusions about existing components in the water (e.g., as an index of phytoplankton biomass in clearest waters) can also be drawn. Both data sets are needed as a reference for hyperspectral radiometric observations, as one goal is the determination of ocean color by radiometric measurements (compare Garaba et al, 2014). Analysis is still in progress.

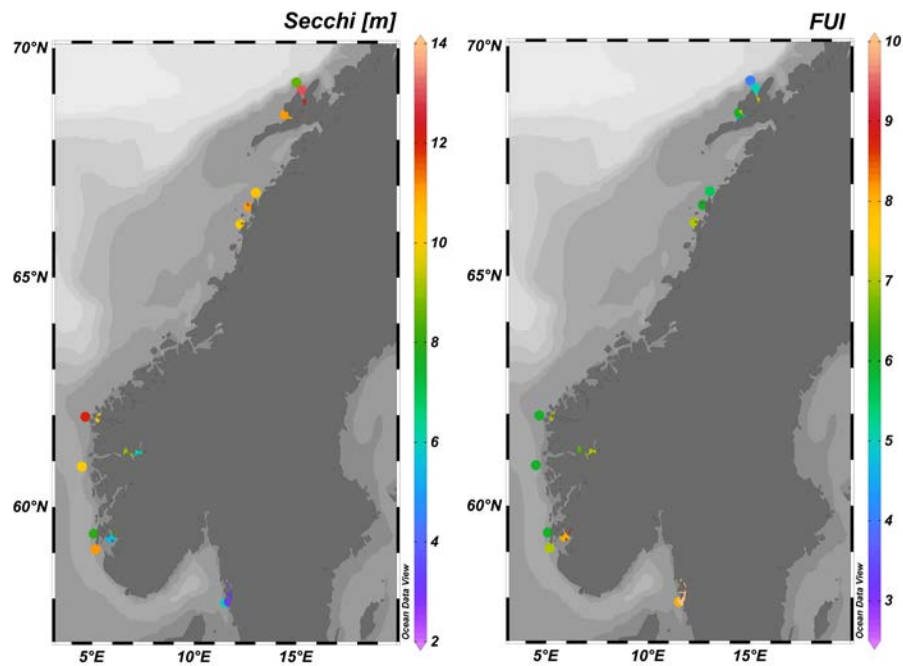


Figure 22 Measured Secchi depths at daytime and Forel-Ule indices (FUI) determined for all stations along the Norwegian and Swedish coast.

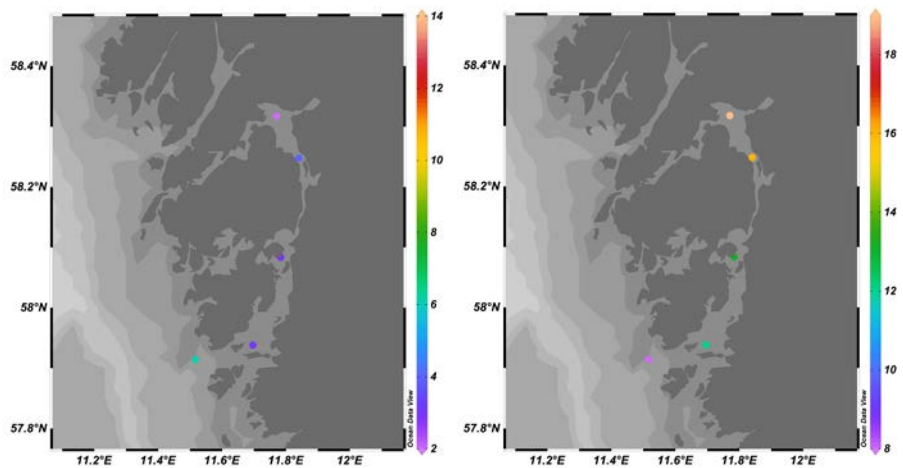


Figure 23 Secchi depths and Forel-Ule indices (FUI) determined for the Swedish stations during daytime. An inverse relationship can be clearly seen.

6.2 Nutrients and DOM

(Westphal, Burau, Krock)

Nutrients

Nutrient analysis performed from five depths at all CTD stations showed that macro-nutrients were almost depleted at the surface. Nitrate concentrations at the surface were $< 2.5 \mu\text{M}$, nitrate $< 0.2 \mu\text{M}$, silicate < 3.5 , phosphate < 0.4 and ammonium $< 1 \mu\text{M}$. At station 31 at 15 m a higher silicate ($18 \mu\text{M}$) and ammonium ($1.2 \mu\text{M}$) concentration were measured. The concentrations increased with depth (Figure 22- Figure 26), which is typical for the late summer (nitrate $< 13.9 \mu\text{M}$, silicate $< 20 \mu\text{M}$ and up to $25.2 \mu\text{M}$ at station 31, phosphate $< 1 \mu\text{M}$ and up to $1.84 \mu\text{M}$ at station 31. The nitrate/phosphate ratio followed (almost ideally) the Redfield ratio (not shown), except for the most northerly transect Lofoten and most southernly transect in Sweden waters. Water layers of the Lofoten, Nordfjord and Sognefjord showed a high stratification, which is likely due to river water runoff. In this region, nutrients were also variable with depth due to the complex hydrographic and topographic structure. In Stavanger Fjord and the Swedish fjord area nutrients were generally low throughout the water column (nitrate $< 3.2 \mu\text{M}$ but bottom water up to $9 \mu\text{M}$, nitrite < 1.2 , silicate $< 4 \mu\text{M}$ but bottom water up to $25.2 \mu\text{M}$ at station 31, phosphate $< 0.9 \mu\text{M}$, ammonium $< 2 \mu\text{M}$), as is typical for the season. Basic chemical relationships will be further investigated and data will be used for the interpretation of the biological data, in particular the phytoplankton distribution.

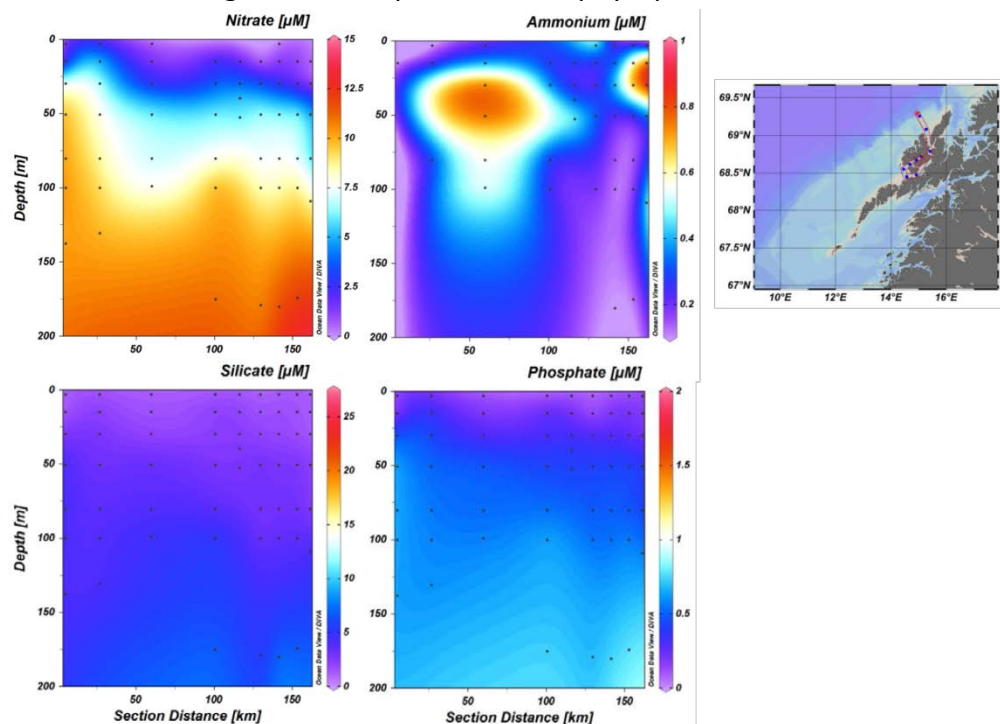


Figure 24 Map of the investigated Lofoten area and associated nutrients (nitrate [μM], ammonium [μM], silicate [μM], phosphate [μM]) over the section distance (km) (from outside to inside stations). Nutrients are shown over the full depth.

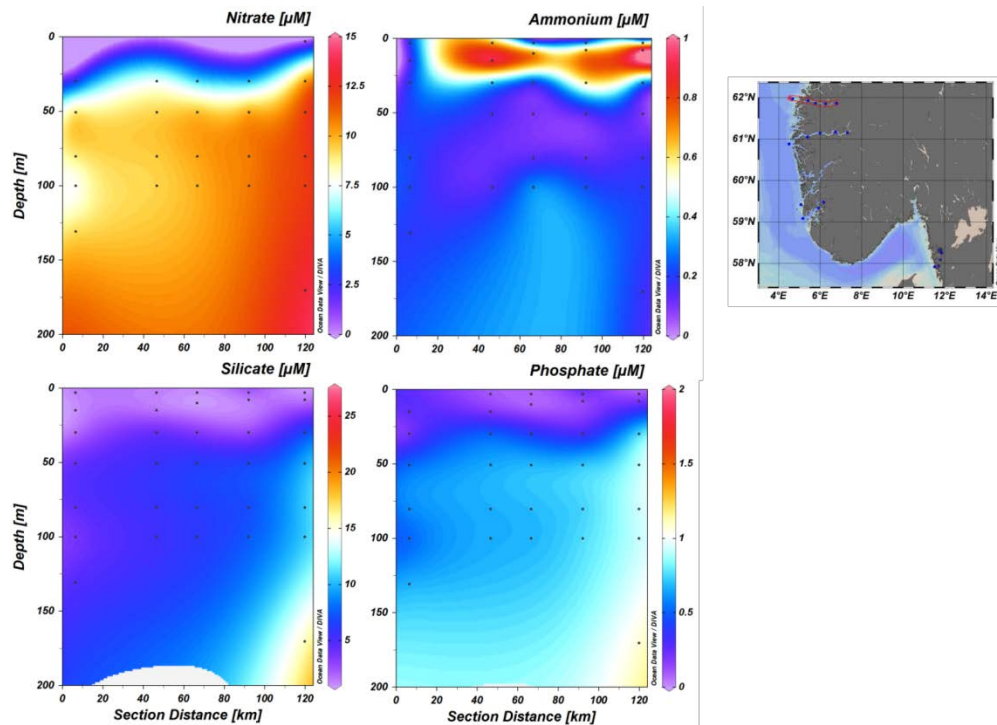


Figure 25 Map of the investigated Nordfjord area and associated nutrients (nitrate [μM], ammonium [μM], silicate [μM], phosphate [μM]) over the section distance (km) (from outside to inside stations). For comparison, nutrients are shown for the upper 200 m.

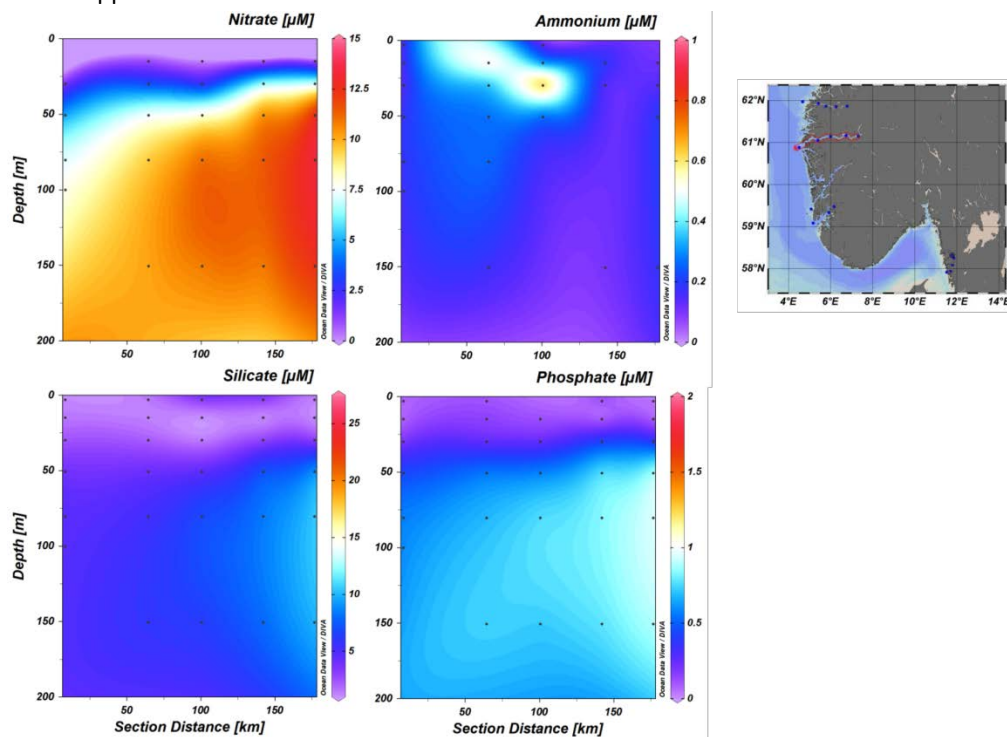


Figure 26 Map of the investigated Sognefjord area and associated nutrients (nitrate [μM], ammonium [μM], silicate [μM], phosphate [μM]) over the section distance (km) (from outside to inside stations). For comparison, nutrients are shown for the upper 200 m.

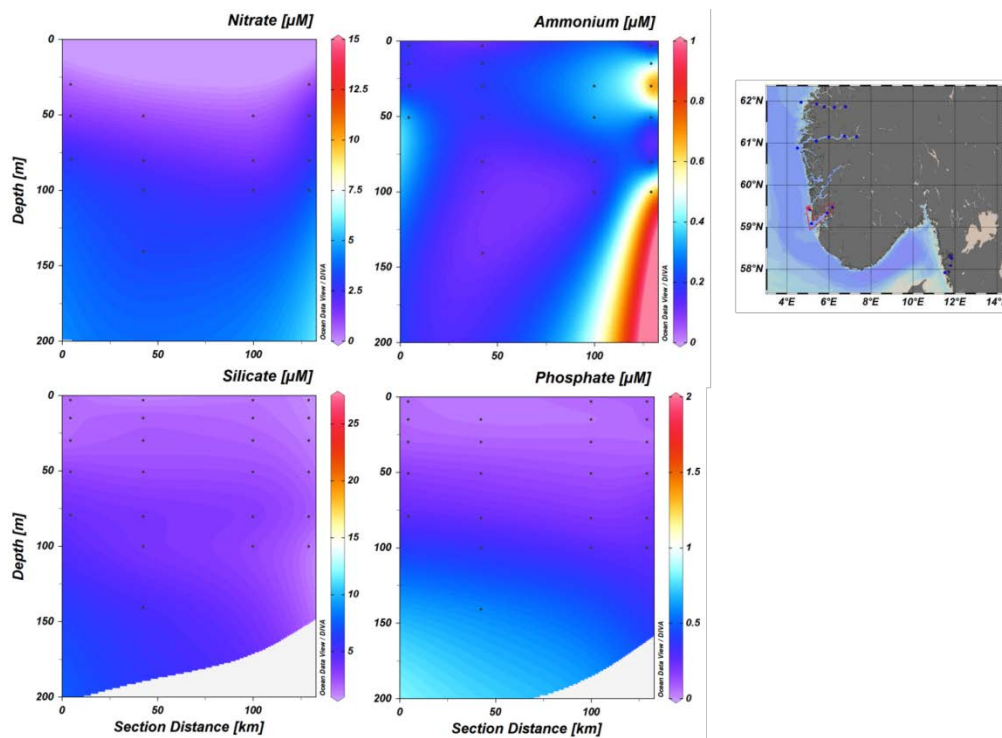


Figure 27 Map of the investigated Stavanger Fjord area and associated nutrients (nitrate [μM], ammonium [μM], silicate [μM], phosphate [μM]) over the section distance (km) (from outside to inside stations). For comparison, nutrients are shown for the upper 200 m.

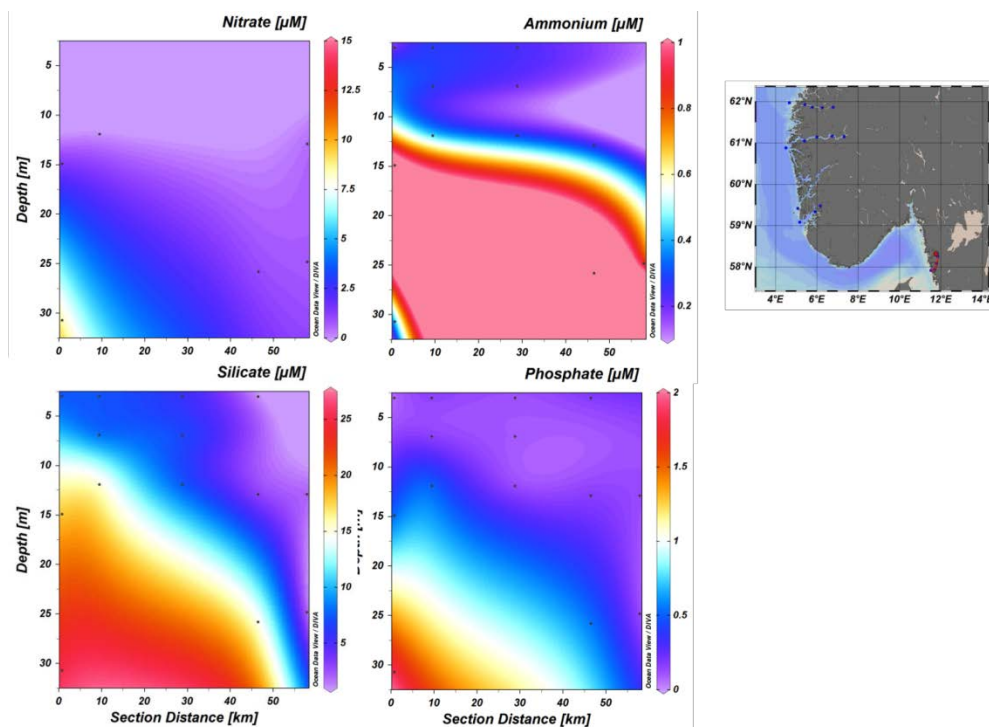


Figure 28 Map of the investigated Swedish fjord area and associated nutrients (nitrate [μM], ammonium [μM], silicate [μM], phosphate [μM]) over the section distance (km) (from outside to inside stations).

DOC concentration and molecular DOM analyses

DOC and DOM samples were pooled from 3 depths (3m, 15m and 30m) for interpretation of the biological data, in particular the phytoplankton distribution. For most samples, the DOC concentration varied between 49-95 μM (Figure 27). Higher concentrations were found in Stavanger Fjord and within Swedish fjord area (107 – 225 μM). Generally, the mixed-surface layer DOC concentration was higher than in the deeper water samples. The values reflected primary production in the surface layer, with more reworked and depleted organic material in deeper waters. The dataset was in good agreement with earlier studies in the North Atlantic, such as the WOCE sections.

Molecular DOM analyses are still part of the ongoing work.

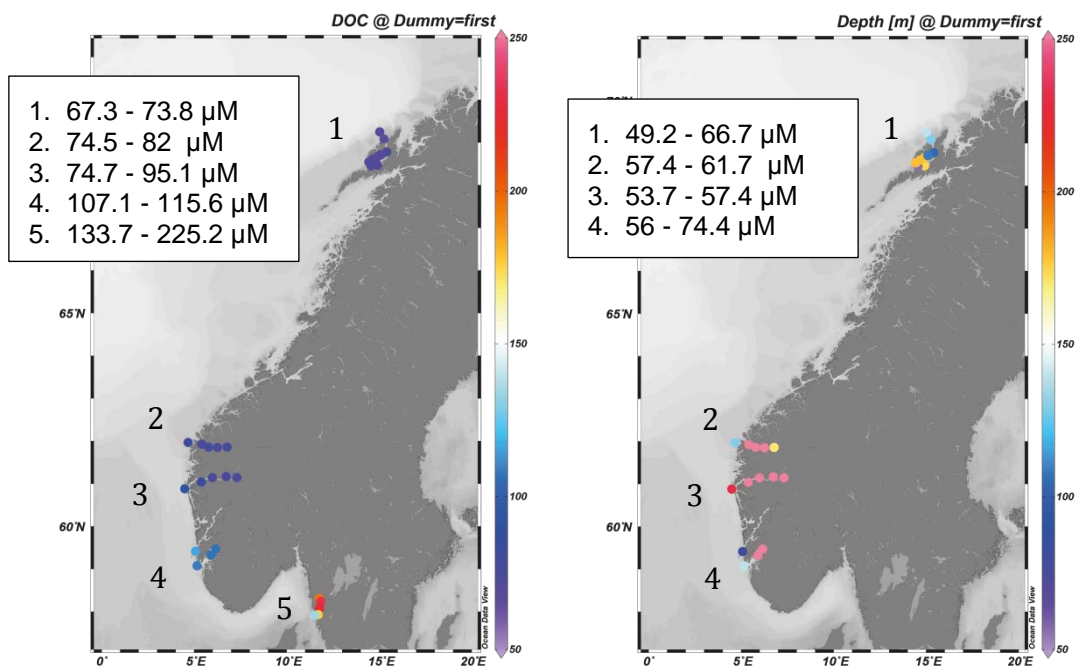


Figure 29 DOC values of the mixed surface sample (3m, 15m and 30m; LEFT) and bottom sample (RIGHT) at all sampling transects. 1 = Lofoten, 2 = Nordfjord, 3 = Sognefjord, 4 = Stavanger Fjord, 5 = Swedish fjord area.

6.3 Toxins in field samples

(Müller, Haslauer, Cembella, Krock)

Toxin profiles differed among the regions (Figure 30). Overall Toxin concentrations were highest in the Sognefjord (1000 – 7000 ng/net tow), followed by the Swedish sampling area (400 – 800 ng/net tow). Within the Lofoten domoic acid was the most relative abundant toxin, but towards the end of the fjord (station 7-9) also dinophysis toxins and pectenotoxins became more relative abundant. For the Nordfjord and Sognefjord dinophysis toxins and pectenotoxins were the dominant toxins. However, toxin concentrations were very low within the Nordfjord. Next to these toxins a higher concentration of spirolides was measured within the Swedish sampling area, with a rising relative abundance towards the end of the transect.

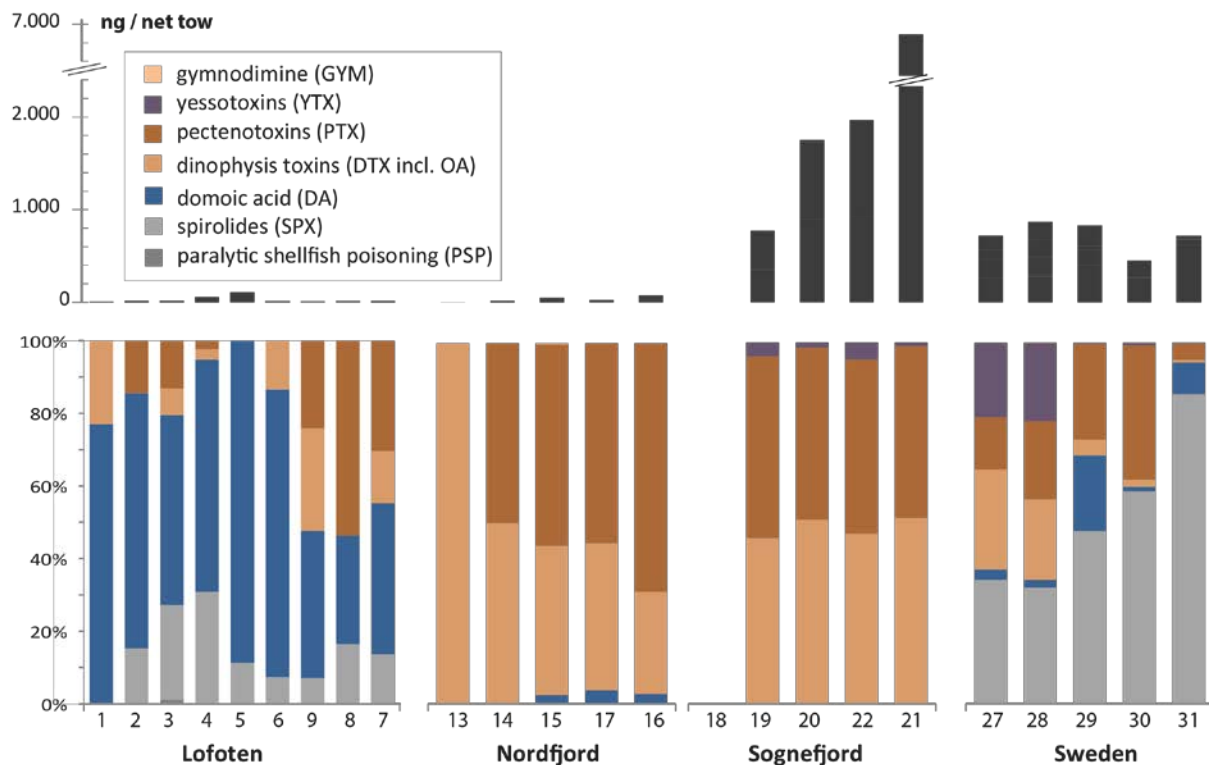


Figure 30 TOP: Toxin concentration [ng/net tow] for the four sampling transects Lofoten (stations 1-9), Nordfjord (stations 13-16), Sognefjord (stations 18-21) and Sweden (stations 27-31). BOTTOM: Toxin profiles for the same transects. PSP comprise GTX3, Neo STX and STX, Dinophysis toxins comprises DTX and OA, and Pectenotoxins PTX2 and PTX12.

6.4 Microplankton species diversity

(Cembella, Murray, Fabro)

Identification and counting of the 20 - 50 μm size-fraction plankton composition from vertical net tows showed dominance of diatoms and dinoflagellates in 70% and 30% of the samples,

respectively. Among the diatoms, the dominant genera were *Chaetoceros*, *Pseudo-nitzschia*, *Corethron*, *Paralia*, *Thalassionema*, *Rhizosolenia* and *Leptocylindrus minimus*. Maximum abundances (7×10^4 cells ml⁻¹ of net concentrate) were reached by the toxigenic genus *Pseudo-nitzschia*.

In approximately half of the samples dominated by dinoflagellates, *Protoperidinium* spp. were most abundant in terms of total cell concentration. Nevertheless, *Ceratium furca*, *Lingulodinium polyedrum*., *Alexandrium* spp., and *Prorocentrum micans* were also dominant at one station each. Maximum abundance (10.4×10^3 cells ml⁻¹ of net concentrate) was reached by *L. polyedrum*.

Putatively toxic dinoflagellates were frequently found in the net samples, although never in high cell abundances (except for *Lingulodinium*). The following table shows the potentially toxic species found and the total number of stations (total = 30) at which they were detected in net tows.

Table 1: Most prominent taxa identified during the cruise and the corresponding station

Taxa	N° of stations
<i>Dinophysis rotundata</i>	27
<i>Dinophysis acuminata</i>	23
<i>Alexandrium</i> spp.	20
<i>Dinophysis acuta</i>	17
<i>Dinophysis norvegica</i>	15
<i>Lingulodinium polyedrum</i>	13
<i>Protoceratium reticulatum</i>	4
<i>Dinophysis ovum</i>	3
<i>Prorocentrum lima</i>	2

6.5 Molecular biodiversity

(Westphal, Kühne John)

Sequencing of three size fractions resulted in a wide range of sequencing depth after quality filtering (4244 - 22354 sequences) and OTUs (334 - 903 OTU). The overlaps of the total of 3,437 OTUs between the size classes are shown in Figure 28. Most OTUs were shared between the nano- and picoplankton (930), followed by unique picoplankton OTUs (703) and shared OTUs between all size fractions (526).

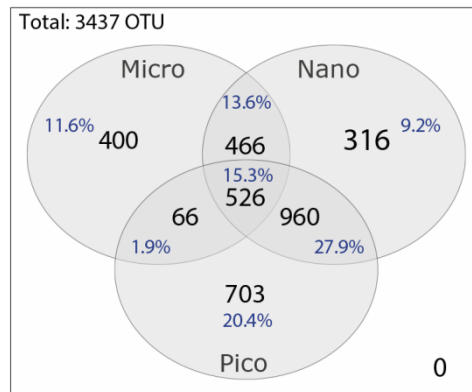


Figure 32 Venn diagram of OTU intersections between the three different size classes: microplankton (20 – 50 μm), nanoplankton (3 – 20 μm) and picoplankton (0.2 – 3 μm). OTUs were generated under a threshold of 98% similarity.

Diversity indices were calculated and are shown in boxplots (Figure 29). The common inverse Simpson’s diversity index was calculated for each size fraction and sampling transects. The microplankton and picoplankton were very similar in all sampling areas. The nanoplankton within the Lofoten, Nordfjord and Sognefjord were significantly more diverse compared to the Swedish coastal and fjords (t-test; p-value < 0.05) and micro-/picoplankton (t-test; p-value < 0.05).

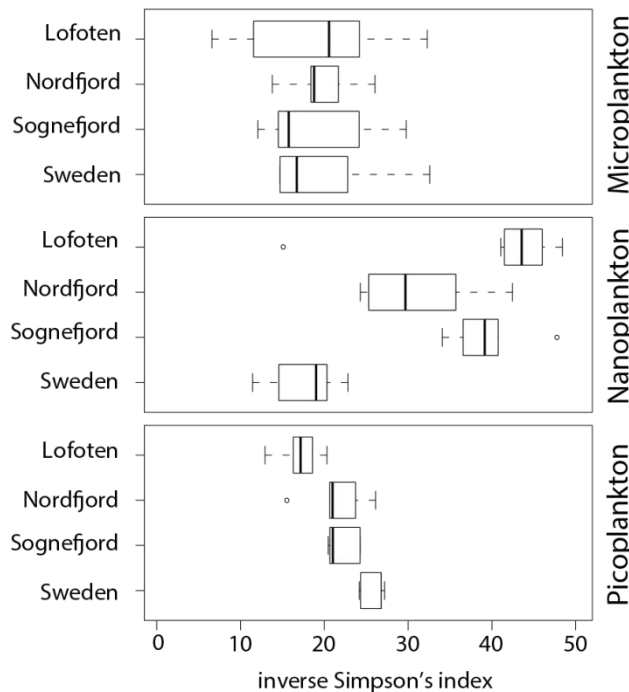


Figure 33 Boxplot comparing the range of diversity of OTUs on genus level across various groups. Each boxplot shows the distribution of the inverse Simpson’s index within one sampling transect and size fraction. Calculations suggest a higher diversity in the nanoplankton (3 – 20 μm) for the Lofoten, Nordfjord and Sognefjord. Lofoten (n = 9), Nordfjord, Sognefjord and Sweden (n = 5). Top, middle and bottom lines of boxes represent the 25th (lower range), 50th (median) and 75th (upper range) percentiles; whiskers represent the non-extreme sample minimum and maximum; points represent outliers.

In Figure 32 and Figure 33 the relative abundance of different OTUs were grouped according their major phylogenetic groups: Alveolata, Haptophyta, Metazoa, Viridiplantae and Stramenopiles for each size fraction. Both Alveolates and Stramenopiles covered 67% of the richness of the total community. Other groups that covered 23% and 11% of the reads could not be assigned.

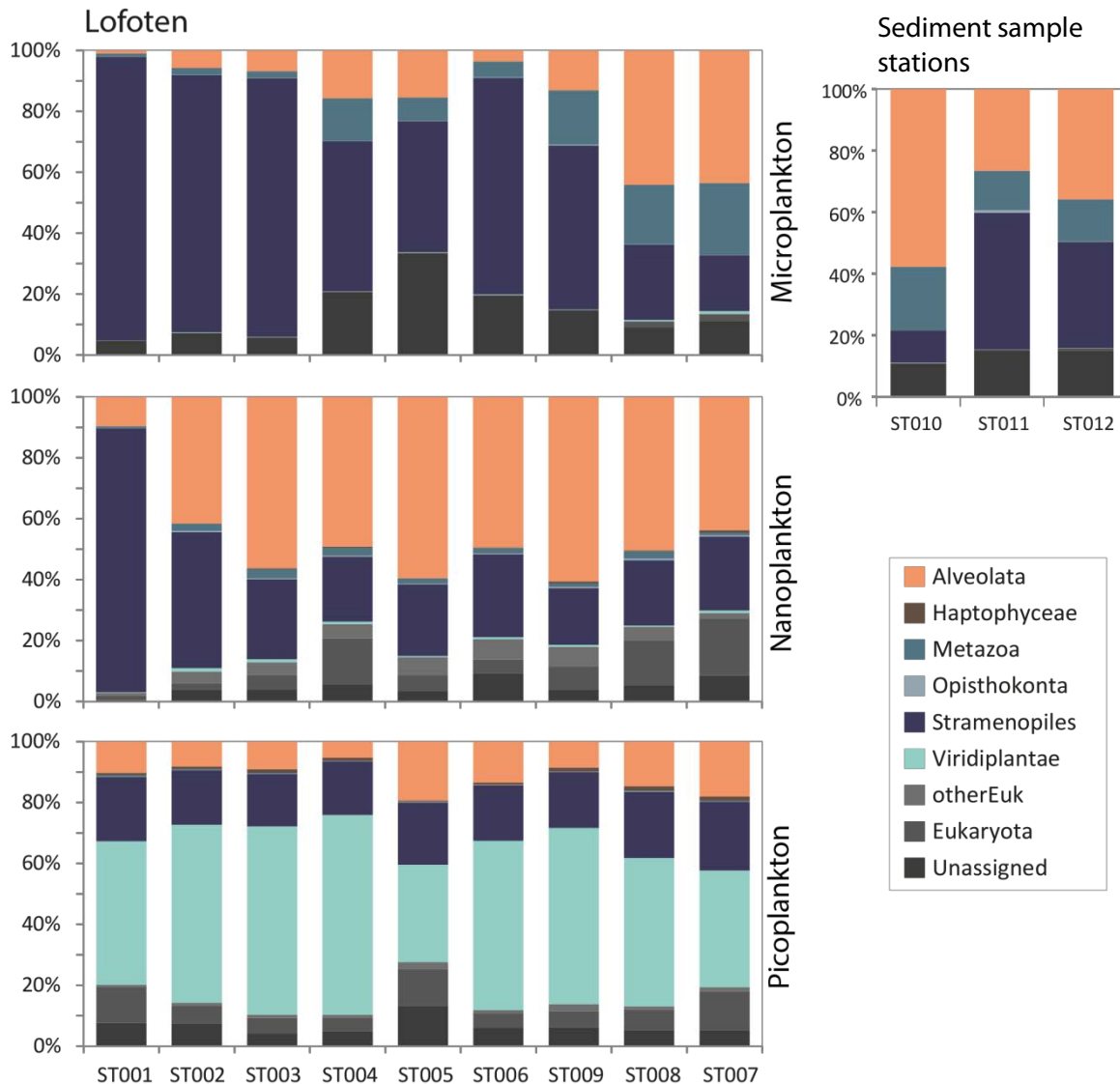


Figure 16 Relative abundance of main taxonomic groups obtained by 454-pyrosequencing and taxonomic assignment at 98% similarity level within the Lofoten sampling transect (LEFT) and the 3 sediment sampling stations (RIGHT). “Other Euk” are eukaryotic groups that comprised < 1% of the total sequences.

The distribution of the main phylogenetic groups within the Lofoten (Figure 32) differed among size fractions as well as along the sampling transect. The dominant group within the microplankton was the stramenopiles (main group = diatoms), but along the sampling transect the alveolates (main group = dinoflagellates) became relatively more abundant in terms of

species diversity. This latter group also showed higher relative abundance within the nanoplankton. ST001 showed a profile dominated by stramenopiles, which may be due to the open ocean location of this station, and thereby was influenced by mixing of different water masses. The Viridiplantae were the main phylogenetic group within the picoplankton.

For Nordfjord and Sognefjord (Figure 33) the number of unassigned sequences within the microplankton increased along the fjord transects, suggesting that some taxonomic groups are missing in the data-base. The distribution of groups in Swedish coastal waters differed from the two Norwegian fjords. Here within the microplankton from Swedish stations more alveolates were present compared to stramenopiles but vice versa for the nanoplankton. For the picoplankton the main groups were more even distributed along the Sognefjord and Swedish fjord system compared to the Nordfjord.

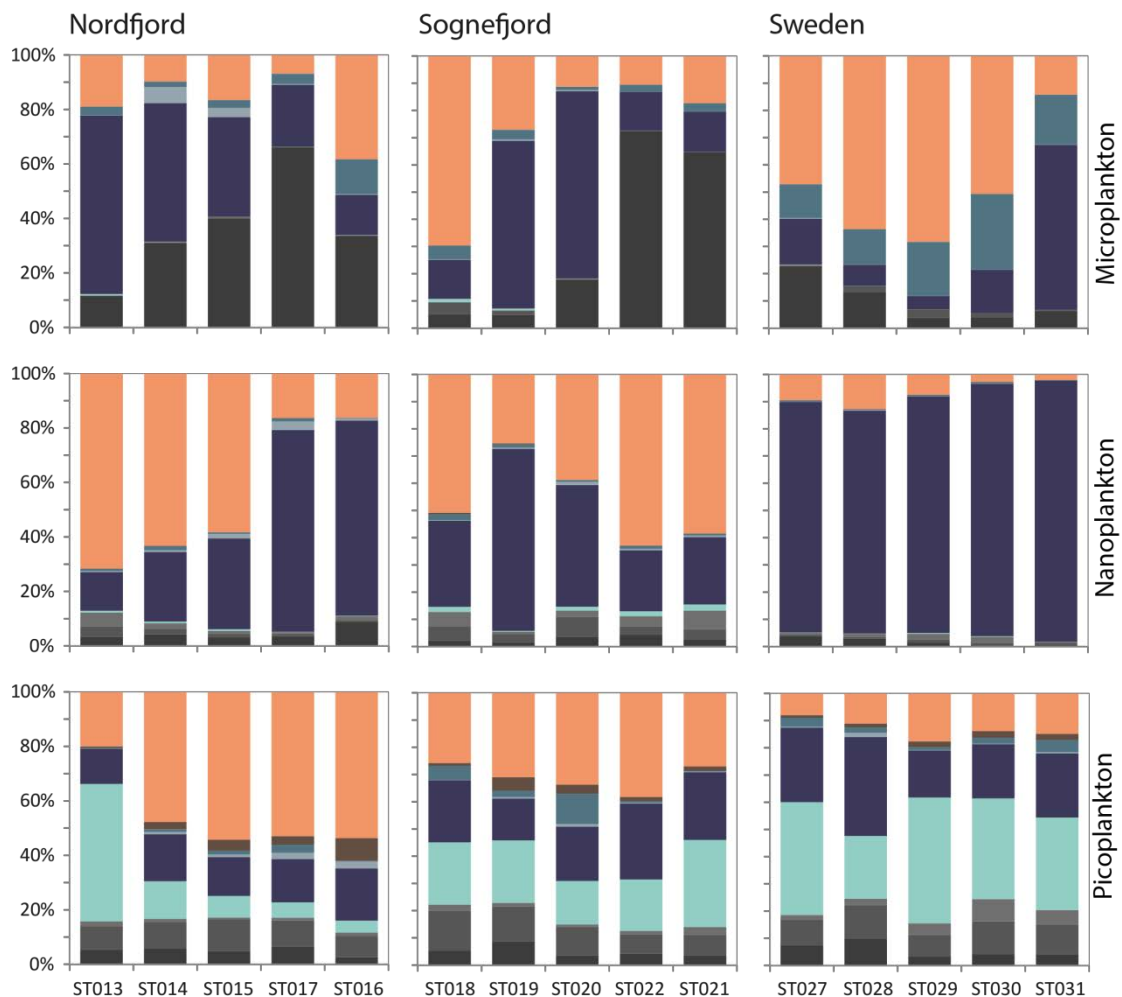


Figure 17 Relative abundance of main taxonomic groups obtained by 454-pyrosequencing and taxonomic assignment at 98% similarity level within Nordfjord, Sognefjord and the Swedish fjord system. The colors follow the color code shown in Figure 30. “Other Euk” are eukaryotic groups comprising < 1% of the total sequences.

Multivariate analysis of the biodiversity

Comparing the similarity of all samples in a NMDS (Figure 34) resulted in a separation of the micro-, nano- and picoplankton but with no clear separation of the sampling transects. A higher similarity of the community with smaller size fraction was observed. Plotting each size fraction in one NMDS plot (Figure 33) resulted in a separation of the sampling transects. Within the microplankton fraction, sampling transects indicate a partitioning by different environmental parameters. Salinity and temperature are negatively correlated and separate the Lofoten and Swedish fjord systems from each other significantly ($p < 0.05$). Same is true for silicate/Chl a and oxygen. Nitrate and the depth of sampling stations (Bot.Depth) show a significant ($p < 0.05$) positive influence on the Nordfjord and Sognefjord community. No significance ($p < 0.05$) was observed by fitting environmental parameters to the nanoplankton and picoplankton NMDS. For both size fractions, the plankton community of Sognefjord, Nordfjord and Lofoten showed a higher similarity to each other than to the Swedish fjord system community. In general the similarity of the community within one sampling transect was higher for smaller size-fractions.

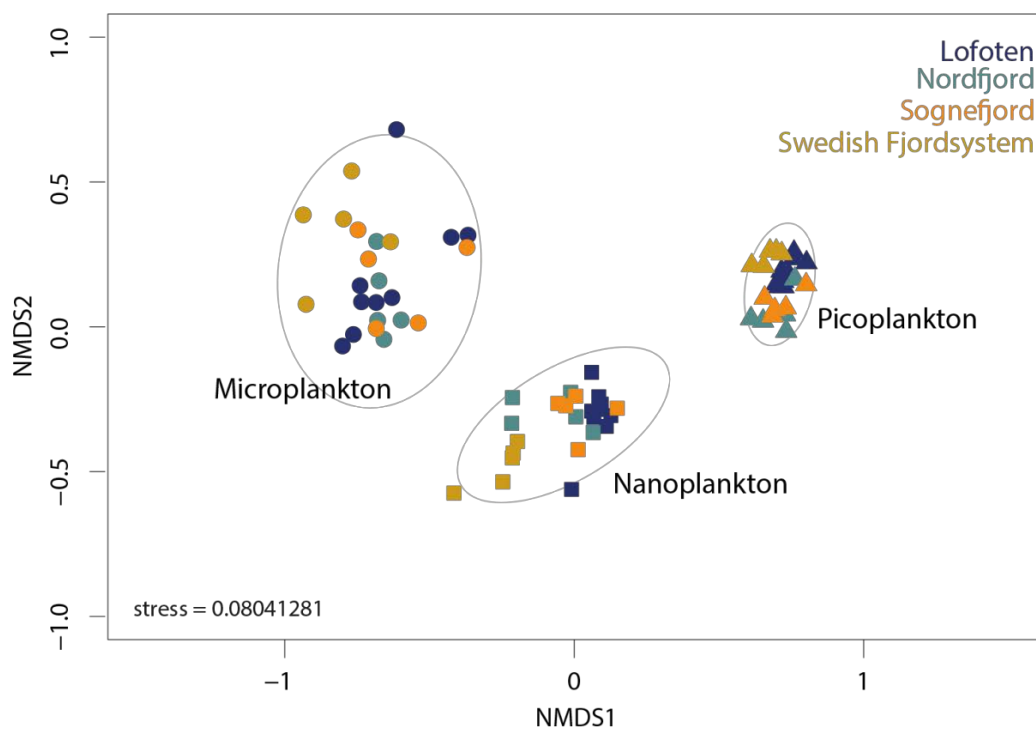


Figure 18 Non-metric multidimensional scaling (NMDS) biplot of a Bray-Curtis dissimilarity matrix of the microplankton (20–50 μm , circles), nanoplankton (3–20 μm , squares) and picoplankton (0.2–3 μm , triangles) OTU abundance data are shown with assigned taxonomy at genus or lower taxonomic level. Species abundance data were normalized with the Hellinger transformation. Ellipses were drawn at 95% confidence limit for all stations from one size fraction. Environmental parameters were fitted to the NMDS plot after normalization and standardization but did not show significance ($p > 0.05$).

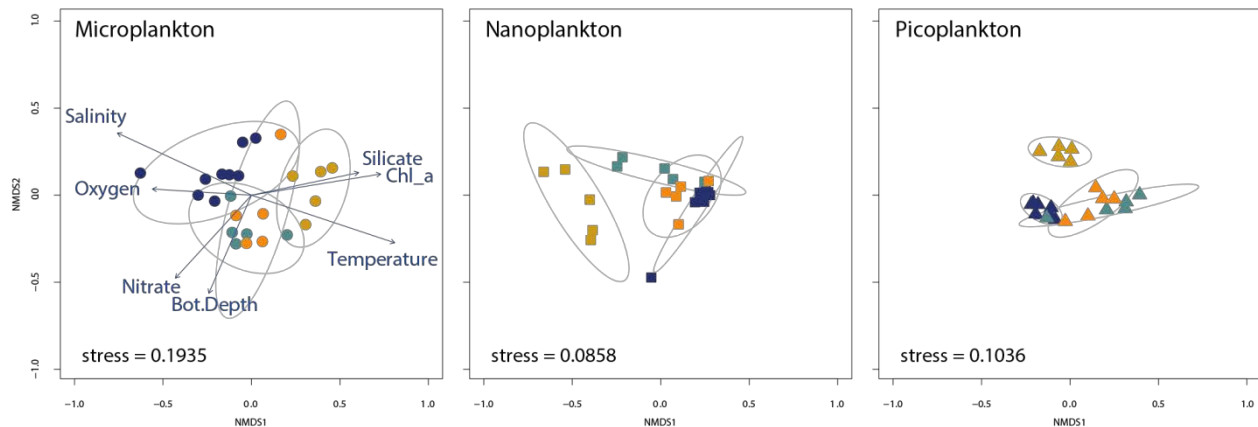


Figure 19 Non-metric multidimensional scaling (NMDS) biplot of a Bray-Curtis dissimilarity matrix of the separate microplankton (20 – 50 μm , circles), nanoplankton (3 – 20 μm , squares) and picoplankton (0.2 – 3 μm , triangle) OTU abundance data are shown with assigned taxonomy at genus or lower taxonomic level. Species abundance data was normalized with the Hellinger transformation. Ellipses were drawn at 95% confidence limit for all stations from one sampling area. The color code for the sampling transects follow the color code in Figure 32. Environmental parameters were fitted to the NMDS plot after normalization and standardization but did not show significance ($p < 0.05$) for the nano- and picoplankton.

6.6 Cyst distribution

(Allan Cembella)

Sediment samples were successfully collected from selected stations along the cruise track both within the fjord systems and along the inner coast. The samples were processed in a preliminary way (as described in Section 5.8) and examined microscopically on board for the presence of *Alexandrium* cysts. At all stations sampled, the granulometric composition of the surface sediments was biased towards fine sand or silt, and little gravel or small rocks were encountered. Such substrates are typically ideal for dinoflagellate cyst accumulation and retention. Nevertheless, throughout the entire sediment sampling regime, *Alexandrium* cysts were extremely rare (typically < 2 cysts cm^{-3} of flocculent sediment slurry) and thus did not warrant further onboard attempts to isolate cysts into culture.

Given the ideal nature of the substrate for cyst deposition, this paucity of *Alexandrium* cysts was rather unexpected. One plausible explanation is that we arrived on station well after major excystment of seed beds (typically May/June) and resulting pelagic blooms may either have been of low magnitude or have been advected away from the fjords – hence yielding only minimal fresh cyst deposition. Support for this suggestion is provided by the fact that cyst concentrations of other large thecate dinoflagellates known to form cyst deposits were also very low in all samples. The dominant taxa identified corresponded to cysts of *Scrippsiella* sp., *Lingulodinium polyedrum*, *Protoceratium reticulatum* and *Protoperidinium* spp. – all of these were commonly found in sediments but never in high abundance (< 50 cysts cm^{-3} flocculent layer slurry). Again these were the most dominant dinoflagellate species present as vegetative cells in the pelagic

zone as recovered via net tows. Sediment samples are archived for further analysis of granulometric properties but this is probably not justified given the low abundance of *Alexandrium* cysts.

6.7 Metatranscriptomics

(Wohlrab and John)

The assembly of the metatranscriptome resulted in a total of ~ 3million contigs that could be assigned to 320 different species. Comparison of the metatranscriptomic information from e.g. the region of the Lofoten with the fjord system in Sweden (Orust) showed that the activity of the phytoplankton based on their transcriptome at the Lofoten region was dominated by members of the phylum Bacillariophyta whereas the Swedish fjord system was dominated by Dinophyta (Figure 36). These results reflect the biodiversity patterns obtained from the respective areas (see Figure 31). The results from the metatranscriptome study are currently evaluated in more detail.

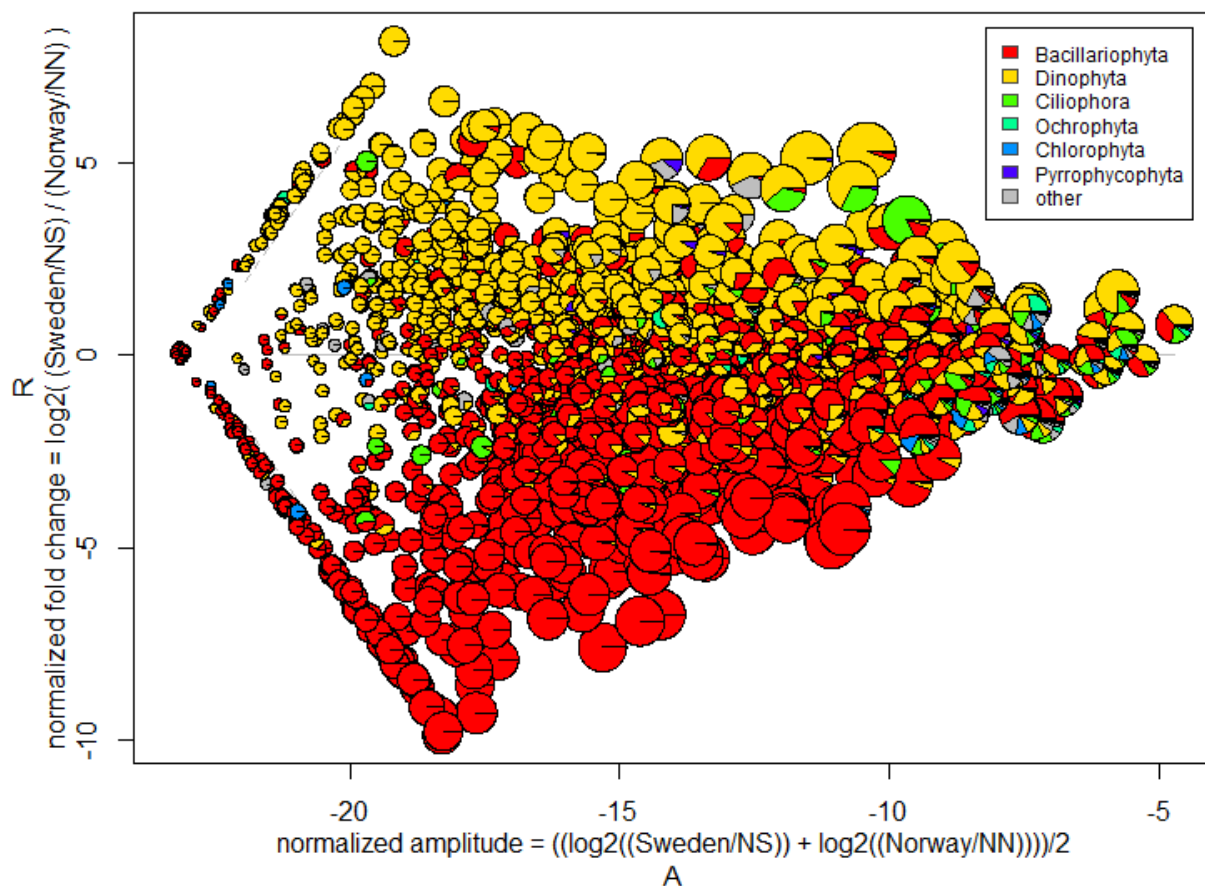


Figure 36 Microbial Abundance Normalized Transcript Analysis Ratio-Average plot showing the differential gene expression of the plankton community from the Swedish fjord system in comparison to the Lofoten region. The circle represents a collection of contigs assigned to a predicted gene function. Circle area fills represent the taxonomic affiliation of the contigs. Plotted are fold-change ratios (R) and the average of read counts (A).

6.8 Viruses

(Kegel)

Sequencing of the mcp region was performed unidirectionally resulting in ~ 161,000 sequences for 16 stations. The number of sequences for each station ranged between 5715 to 15819. Preliminary results of the Sognefjord (stations 18-22) and the Swedish fjord (stations 27-31) showed that > 50% of the sequences are uncultured or unknown Phycodnaviruses, or had no significant BLAST hit (Figure 37). The majority of the identified Chlorophyte viruses with a 97% sequence similarity are *Micromonas pusilla* viruses. Our main interest was in the haptophyte viruses, which were less than 10% of the total OTUs.

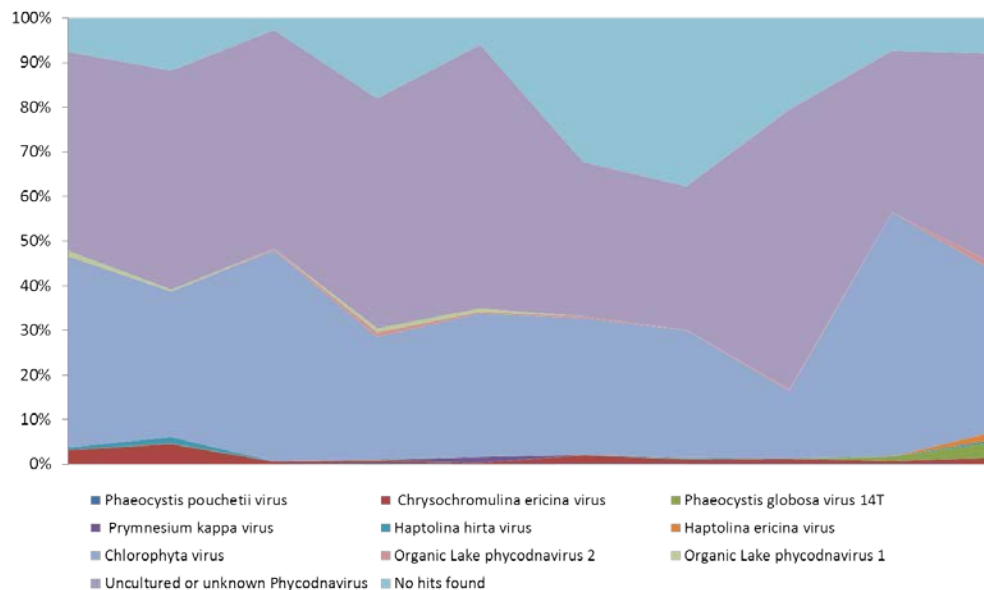


Figure 20 Percentage of sequence reads per OTU of dsDNA Phycodnaviruses.

A canonical correspondence analysis (CCA) shows a trend of separation of the *Haptolina ericina* virus and the *Phaeocystis globosa* virus towards higher availability of the environmental parameters phosphate and silicate (Figure 38).

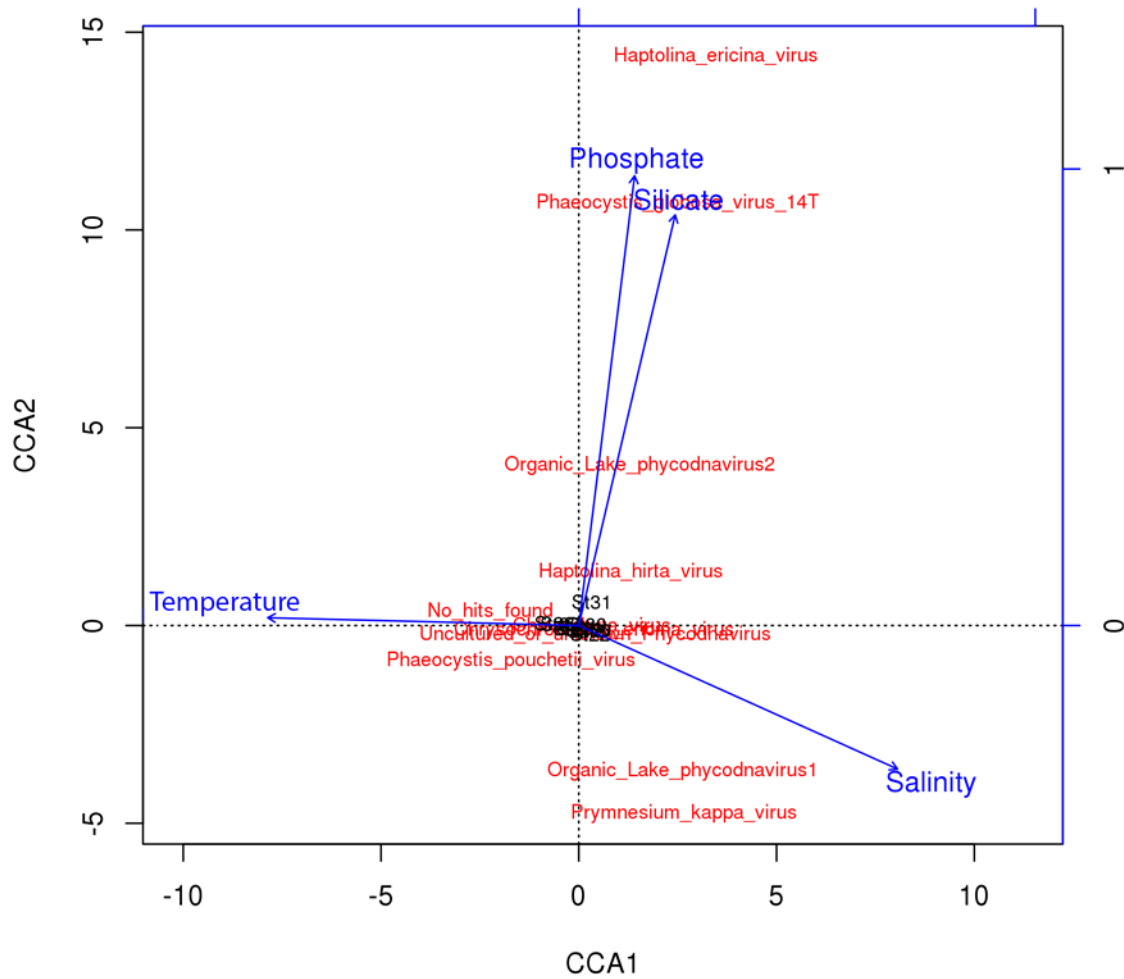


Figure 38 CCA of dsDNA virus fraction from the Sognefjord and the Swedish fjord using a Type I scaling.

Virus isolation

After 14 days of incubation only a sample from station 26 showed a promising lysis of a *P. polylepis* culture. The isolation of potential viruses is still in process.

7 Station List

Station	Datum		Breitengrad	Längengrad	Tiefe
Station	Date		Latitude	Longitude	depth
001	23.08.2014	Lofoten	69° 15,42' N	15° 1,32' E	141.5
002	23.08.2014		69° 4,97' N	15° 16,07' E	134.2
003	24.08.2014		68° 47,19' N	15° 24,36' E	101.6
004	24.08.2014		68° 28,43' N	14° 54,77' E	190.1
005	24.08.2014		68° 27,16' N	14° 33,38' E	56.0
006	24.08.2014		68° 33,00' N	14° 26,86' E	182.8
007	25.08.2014		68° 42,93' N	15° 4,90' E	112.6
008	25.08.2014		68° 40,48' N	14° 54,72' E	169.4
009	25.08.2014		68° 36,95' N	14° 40,90' E	187.6
010	26.08.2014		66° 50,86' N	13° 1,39' E	39.0
011	26.08.2014		66° 32,76' N	12° 40,53' E	75.0
012	26.08.2014		66° 9,97' N	12° 15,95' E	41.3
013	28.08.2014	Nordfjord	61° 58,12' N	4° 40,06' E	138.6
014	28.08.2014		61° 55,62' N	5° 25,32' E	423.8
015	28.08.2014		61° 51,93' N	5° 46,84' E	447.6
016	29.08.2014		61° 51,95' N	6° 46,98' E	178.8
017	29.08.2014		61° 51,10' N	6° 15,87' E	411.9
018	30.08.2014	Sognefjord	60° 53,00' N	4° 29,93' E	255.7
019	30.08.2014		61° 2,88' N	5° 23,39' E	509.3
020	30.08.2014		61° 8,59' N	6° 0,00' E	1268.3
021	31.08.2014		61° 8,99' N	7° 18,90' E	818.7
022	31.08.2014		61° 10,07' N	6° 44,40' E	1000.1
023	02.09.2014	Stavanger	59° 25,15' N	5° 4,25' E	149.1
024	03.09.2014		59° 4,93' N	5° 10,09' E	142.8
025	03.09.2014		59° 19,92' N	5° 54,86' E	509.3
026	03.09.2014		59° 28,70' N	6° 9,98' E	368.9
027	05.09.2014	Sweden	57° 54,85' N	11° 30,99' E	24.6
028	05.09.2014		57° 56,30' N	11° 41,77' E	27.6
029	05.09.2014		58° 5,01' N	11° 47,02' E	11.7
030	05.09.2014		58° 14,88' N	11° 50,44' E	16.7
031	06.09.2014		58° 19,03' N	11° 46,24' E	32.3

8 Data and Sample Storage and Availability

All data will be transferred to the PANGAEA database as soon as they are available and quality checked. Depending on data type and progress of sample analysis, this will be done within 2-3 years. Already several datasets were submitted to PANGAEA, allocated by the cruise identifier HE431. The following compilation names the scientists who are responsible for access to the different data and sample sets.

CTD and bio-optics data are held at the ICBM (Oldenburg) and were analyzed by the group of Prof. Dr. O. Zielinski. CTD data and accompanying information were already submitted to PANGAEA.

Nutrient and DOM data are archived at AWI (Bremerhaven) (Prof. Dr. B. Koch, S. Westphal).

Toxin analyses (Dr. B. Krock) were performed by AWI (Bremerhaven) and the results will be uploaded to PANGAEA.

Most algal strains isolated during this cruise are maintained at AWI (Prof. Dr. A. Cembella) and are available on request.

Genomic analysis was performed by AWI (Dr. U. John, Dr. S. Wohlrab, S. Westphal). Information will be stored in the AWI repository and (where applicable) transferred to PANGAEA.

Cyst isolation and distribution data were analyzed by AWI (Prof. Dr. A. Cembella) and will be uploaded to PANGAEA. No resulting cultured isolates are available from cyst derivation due to the low abundance of *Alexandrium* cysts; successful isolation of other species such as *P. reticulatum* and *L. polyedrum* was not necessary from cysts because of the high abundance of vegetative cells from the pelagic zone,

9 Acknowledgements

The scientific team is very grateful to Captain Werner Riederer and crew of the *RV Heincke* for cooperative and efficient assistance with operation and deployment of scientific equipment, and for the friendly and positive working and social atmosphere on board. The HAB research was conducted as part of the IOC/SCOR program on Global Ecology and Oceanography of Harmful Algal Blooms (GEOHAB) within the Core Research Project on HABs in Fjords and Coastal Embayments. The AWI contribution was provided by the HGF Program Earth and Environment under PACES Theme 2 (Coast) Workpackage 3.

10 References

Arar, E.J., Collins, G. B. (1997) EPA Method 445.0 *In Vitro* Determination of Chlorophyll *a* and Phaeophytin *a* in Marine and Freshwater Algae by Fluorescence, Revision 1.2 in: EPA/600/R-97/072 Methods for the Determination of Chemical Substances in Marine and Estuarine Environmental Matrices EPA US.

Coble, P.G. (2007) Marine Optical Biogeochemistry: The Chemistry of Ocean Color, Chemical Reviews, 2007, Vol. 107, No. 2, 407-418

Garaba, S., Zielinski, O. (2013) Comparison of remote sensing reflectance from above-water and in-water measurements west of Greenland, Labrador Sea, Denmark Strait, and west of Iceland, Optics Express, 21 (13), 15938-15950, DOI:10.1364/OE.21.015938.

Baggesen, C., Moestrup, Ø., Daugbjerg, N., Krock, B., Cembella, A.D., Madsen, S. (2012) Molecular phylogeny and toxin profiles of *Alexandrium tamarense* (Lebour) Balech (Dinophyceae) from the west coast of Greenland. Harmful Algae 19, 108-116.

Diener, M., Erler, K., Hiller, S., Christian, B., Luckas, B. (2006) Determination of Paralytic Shellfish Poisoning (PSP) toxins in dietary supplements by application of a new HPLC/FD method. European Food Research and Technology 224, 147-151.

Kattner, G., H. Becker (1991). Nutrients and organic nitrogenous compounds in the marginal ice zone of the Fram Strait. J. Mar. Syst. 2: 385-394

Krock, B., Seguel, C.G., Cembella, A.D. (2007) Toxin profile of *Alexandrium catenella* from the Chilean coast as determined by liquid chromatography with fluorescence detection and liquid chromatography coupled with tandem mass spectrometry. Harmful Algae 6, 734-744.

Krock, B., Tillmann, U., Alpermann, T.J., Voß, D., Zielinski O., Cembella, A.D. (2013) Phycotoxin composition and distribution in plankton fractions from the German Bight and western Danish coast. J. Plank. Res. 35, 1093-1108.

Preston-Thomas, H. (1990) The international temperature scale of 1990 (ITS-90). Metrologia 27, 3-10.